

1 **Global scale evaluation of precipitation datasets for**  
2 **hydrological modelling**

3 Solomon H. Gebrechorkos<sup>1,2</sup>, Julian Leyland<sup>2</sup>, Simon J. Dadson<sup>1</sup>, Sagy Cohen<sup>3</sup>, Louise Slater<sup>1</sup>,  
4 Michel Wortmann<sup>1</sup>, Philip J. Ashworth<sup>4</sup>, Georgina L. Bennett<sup>5</sup>, Richard Boothroyd<sup>6</sup>, Hannah  
5 Cloke<sup>7,8</sup>, Pauline Delorme<sup>9</sup>, Helen Griffith<sup>7</sup>, Richard Hardy<sup>10</sup>, Laurence Hawker<sup>11</sup>, Stuart  
6 McLelland<sup>9</sup>, Jeffrey Neal<sup>11</sup>, Andrew Nicholas<sup>5</sup>, Andrew J. Tatem<sup>2</sup>, Ellie Vahidi<sup>5</sup>, Yinxue Liu<sup>1</sup>,  
7 Justin Sheffield<sup>2</sup>, Daniel R. Parsons<sup>10</sup>, Stephen E. Darby<sup>2</sup>

8 <sup>1</sup>School of Geography and the Environment, University of Oxford, Oxford, UK

9 <sup>2</sup>School of Geography and Environmental Science, University of Southampton, Southampton, SO17 1BJ, United  
10 Kingdom

11 <sup>3</sup>Department of Geography and the Environment, University of Alabama, Tuscaloosa, AL, USA

12 <sup>4</sup>School of Applied Sciences, University of Brighton, Sussex, BN2 4AT

13 <sup>5</sup>Department of Geography, Faculty of Environment, Science and Economy, University of Exeter, Exeter, EX4  
14 4RJ, United Kingdom

15 <sup>6</sup>School of Geographical & Earth Sciences, University of Glasgow, UK

16 <sup>7</sup>Department of Geography and Environmental Science, University of Reading, UK

17 <sup>8</sup>Department of Meteorology, University of Reading, UK

18 <sup>9</sup>Energy and Environment Institute, University of Hull, Hull, United Kingdom

19 <sup>10</sup>Department of Geography, Durham University, Lower Mountjoy, South Road, Durham, DH1 3LE

20 <sup>11</sup>School of Geographical Sciences, University of Bristol, Bristol, BS8 1SS, UK

21 *Correspondence to:* Solomon H. Gebrechorkos ([solomon.gebrechorkos@ouce.ox.ac.uk](mailto:solomon.gebrechorkos@ouce.ox.ac.uk))

22 **Abstract.** Precipitation is the dominant driver of the hydrological cycle but it is challenging to accurately  
23 measure at suitably high resolution over global scales using satellites and models. Here, we assessed the  
24 performance of six global and quasi-global high-resolution precipitation datasets (European Center for Medium-  
25 range Weather Forecast (ECMWF) Reanalysis version 5 (ERA5), Climate Hazards group Infrared Precipitation  
26 with Stations version 2.0 (CHIRPS), Multi-Source Weighted-Ensemble Precipitation version 2.80 (MSWEP),  
27 TerraClimate (TERRA), Climate Prediction Centre Unified version 1.0 (CPCU) and Precipitation Estimation from  
28 Remotely Sensed Information using Artificial Neural Networks-Cloud Classification System-Climate Data  
29 Record (PERCCDR)) for hydrological modelling globally and quasi-globally. We forced the WBMsed global  
30 hydrological model with the precipitation datasets to simulate river discharge from 1983 to 2019 and evaluated  
31 the predicted discharge against 1825 hydrological stations worldwide, using a range of statistical methods. The  
32 results show large differences in the accuracy of discharge predictions when using different precipitation input  
33 datasets. Based on evaluation at annual, monthly and daily time scales, MSWEP followed by ERA5 demonstrated  
34 a higher CC and KGE than other datasets for more than 50% of the stations. Whilst ERA5 was the second-highest  
35 performing dataset, it exhibited the highest error and bias in about 20% of the stations. The PERCCDR is the least  
36 well-performing dataset with bias up to 99% and a normalised root mean square error up to 247%. PERCCDR  
37 revealed a higher KGE and CC than the other products in less than 10% of the stations. Even though MSWEP  
38 provided the best performance overall, our analysis reveals high spatial variability, meaning that it is important to  
39 consider other datasets in areas where MSWEP showed a lower performance. The results of this study highlight  
40 the importance of, and provide guidance on, the selection of precipitation datasets for modelling river discharge  
41 for a basin, region or climatic zone, as there is no single best precipitation dataset globally. Finally, the large  
42 discrepancy in the performance of the datasets in different parts of the world highlights the need to improve global  
43 precipitation data products.

44  
45  
46  
47  
48  
49  
50  
51  
52  
53  
54  
55  
56

## 57 1. Introduction

58 Whilst precipitation is one the most important components of the global hydrological cycle and regulates the  
59 climate system (Miao et al., 2019; Sadeghi et al., 2021), it remains one of the most challenging variables to  
60 estimate at a global scale using satellite data and modelling approaches (Michaelides et al., 2009; Kidd and  
61 Levizzani, 2011; Beck et al., 2017a; Ursulak and Coulibaly, 2021). Reliable precipitation data with sufficient  
62 spatial and temporal coverage and accurate representation of extreme events is crucial for various applications.  
63 These include the development of water resource management and planning strategies, hydrological applications  
64 including forecasting hydrological extremes, and climate change analysis (Mehran and AghaKouchak, 2014;  
65 Nguyen et al., 2018; Sadeghi et al., 2021; Acharya et al., 2019). Observed precipitation from meteorological  
66 stations is typically used at local to river basin scale with gauge-based gridded precipitation datasets, such as from  
67 the Global Historical Climatology Network (Menne et al., 2012), developed to study climate and hydrology over  
68 larger scales. However, precipitation from gauges and gauge-based gridded datasets have several drawbacks such  
69 as limited spatial and temporal coverage, prevalence of missing values, and limited accuracy in sparsely populated  
70 and remote areas (Kidd and Levizzani, 2011; Reichle et al., 2011; Kidd et al., 2017; Sun et al., 2018; Gebrechorkos  
71 et al., 2018; Hafizi and Sorman, 2022). In addition, data-sharing policies have caused significant challenges in  
72 obtaining data, particularly in developing countries (Gebrechorkos et al., 2018; Hafizi and Sorman, 2022).

73 Given the challenges in representing precipitation at global scales, satellite, climate model, and reanalysis-based  
74 precipitation datasets can form the basis for monitoring and prediction of water resources and hydrological  
75 extremes, particularly in data-scarce regions of the world (Sheffield et al., 2018; Dembélé et al., 2020).  
76 Nevertheless, uncertainties and errors in these datasets require careful analysis to assess their suitability for a  
77 specific use. Error in satellite-based precipitation estimates can be due to errors in the sensor measurements, the  
78 frequency of sampling, and the retrieval algorithms, including the representation of cloud physics (Dembélé et al.,  
79 2020; Laiti et al., 2018; Alazzy et al., 2017). Climate model-based datasets, including reanalyses, have large  
80 uncertainty due to their coarse spatial resolution and ambiguity associated with model parameters (Gebrechorkos  
81 et al., 2018; AL-Falahi et al., 2020; Dembélé et al., 2020; Her et al., 2019). Reanalysis datasets may correct for  
82 some of these errors via the assimilation of observational data, but this comes with its own uncertainties due to  
83 the error characteristics of the assimilated observations and the assimilation scheme (Sheffield et al., 2006; Parker,  
84 2016). In hydrological modelling, errors and biases in precipitation data result in poor representation of the  
85 hydrological responses and affect applications (Maggioni and Massari, 2018; Zambrano-Bigiarini et al., 2016).  
86 For example, according to Bárdossy et al. (2022), uncertainty in precipitation can lead to hydrological model  
87 errors of up to 50%. Hence, it is important to assess the quality and accuracy of the precipitation products before  
88 using them in global or basin-scale hydrological models. In data-limited regions, hydrological models driven by  
89 precipitation datasets developed from satellite sources, reanalysis or climate models are the only plausible way to  
90 represent the terrestrial water cycle (van Huijgevoort et al., 2013).

91 Over the last few decades, several global and quasi-global precipitation datasets have been developed that address  
92 some of these challenges and can be used to drive hydrological models at regional and global scales. These  
93 precipitation datasets differ in terms of their spatial resolution, spatial coverage (e.g., global or regional), data  
94 sources (e.g., gauge, satellite, reanalysis, and radar), temporal resolution (e.g., sub-daily and daily), and length of

95 record. It is therefore important to evaluate the accuracy of the datasets before they are used to drive global or  
96 regional scale hydrological models. Most studies have evaluated precipitation datasets using observed data from  
97 field-based meteorological stations at a range of scales (e.g., Beck et al., 2017a; Gebrechorkos et al., 2018; Xiang  
98 et al., 2021; Sun et al., 2018; Hong et al., 2022; Wati et al., 2022; AL-Falahi et al., 2020; Ahmed et al., 2019;  
99 Fallah et al., 2020). Hydrological models have also been used to assess the quality of the precipitation dataset by  
100 comparing simulated and observed discharge across different spatial scales (e.g., Mazzoleni et al., 2019; Beck et  
101 al., 2017a; Zhu et al., 2018; Raimonet et al., 2017; Guo et al., 2018; Wang et al., 2020; Salehi et al., 2022; Zhu et  
102 al., 2018; Seyyedi et al., 2015). In principle, this latter approach is able to identify the precipitation datasets which  
103 best represent hydrological variability including extremes, even in catchments where there have been multiple  
104 drivers of change.

105 There are a limited number of studies assessing multiple precipitation datasets for global hydrological model  
106 applications (Voisin et al., 2008; Beck et al., 2017a; Mazzoleni et al., 2019). Voisin et al. (2008) conducted a  
107 global-scale evaluation of two precipitation products for hydrological modelling. Beck et al., (2017a) compared  
108 the performance of 22 precipitation datasets for global hydrological modelling. Mazzoleni et al. (2019) evaluated  
109 18 different precipitation datasets in eight river basins on different continents. Both Beck et al. (2017a) and  
110 Mazzoleni et al. (2019) found that merged satellite-observation precipitation products showed the best  
111 performance compared to satellite-only products. These studies exclusively concentrate on a daily time scale,  
112 evaluating performance solely through the Nash-Sutcliffe Efficiency (NSE). Neither study extends their  
113 assessment to monthly and annual time scales, and notably, they do not assess the hydrological extremes, which  
114 in hydrological terms are considered important to capture. Here, we build upon the work by Beck et al., (2017a)  
115 by adding recently developed high-resolution precipitation datasets. These include the European Centre for  
116 Medium-range Weather Forecast (ECMWF) Reanalysis version 5 (ERA5) (Hersbach et al., 2020), TerraClimate  
117 (Abatzoglou et al., 2018), Precipitation Estimation from Remotely Sensed Information using Artificial Neural  
118 Networks-Cloud Classification System-Climate Data Record (PERCCDR, Sadeghi et al., 2021) and the latest  
119 Multi-Source Weighted-Ensemble Precipitation version 2.80 (MSWEP). These additions significantly broaden  
120 the scope of this study when compared to earlier efforts, offering a diverse range of products with distinct  
121 methodologies. In addition, herein we use multiple statistical metrics to evaluate the performance of the  
122 precipitation products for hydrological modelling at daily, monthly and annual time scales and for daily extremes,  
123 which represents a current gap in the modelling literature.

124 The aim of this study is to undertake a comprehensive evaluation, spanning various temporal and spatial scales,  
125 to examine how different input precipitation datasets impact the predictions of a global hydrological model. We  
126 assess six high-resolution precipitation datasets, each with records spanning over 30 years. A comprehensive and  
127 physically based gridded global hydrological model (WBMsed; Cohen et al., (2013)) is used to simulate river  
128 discharge globally. The objective is not to evaluate the absolute performance of the hydrological model, which  
129 can be influenced by local factors, rather our focus is on comparing the relative performance of the six  
130 precipitation datasets at individual locations. The modelled discharge, derived from the six precipitation datasets,  
131 is assessed across the various time scales by comparing it with observed discharge data collected from 1825 river  
132 gauge stations worldwide. Furthermore, we assess the performance of the precipitation products by examining  
133 their accuracy in representing a range of daily extreme precipitation events. In summary, this research offers a

134 thorough evaluation of a diverse set of precipitation products, spanning from daily extreme events to annual time  
135 scales, providing an invaluable resource for selecting appropriate basin-to-regional-to-global scale inputs for  
136 hydrological modelling applications.

## 137 **2. Data and methods**

138 In the following sections, we outline the various input and evaluation datasets which were used within the  
139 WBMsed hydrological modelling framework. The statistical evaluation methods used to assess the results are also  
140 outlined.

### 141 **2.1. Precipitation datasets**

142 The precipitation datasets used herein are selected based on their length of record (>30 years period), spatial  
143 coverage (global and quasi-global) and recommendations from previous research (Beck et al., 2017a) (Table 1).  
144 Based on the findings of Beck et al. (2017a), datasets with low performance were excluded, while those  
145 demonstrating the highest performance, such as MSWEP and Climate Hazards group Infrared Precipitation with  
146 Stations version 2.0 (CHIRPS), were retained, and new datasets were also incorporated. The selected precipitation  
147 datasets are the ERA5 ERA5, CHIRPS, MSWEP, TerraClimate (TERRA), Climate Prediction Centre Unified  
148 version 1.0 (CPCU), and PERCCDR. Due to their spatial coverage, CHIRPS and PERCCDR are evaluated only  
149 up to latitudes of 50°N and 60°N, respectively (Table 1). Each dataset was subsequently used to force the WBMsed  
150 hydrological model, to generate streamflow estimates. The availability of these datasets with longer records  
151 enables the assessment of long-term hydrological changes at global, regional, and catchment scales.

152 ERA5 is the fifth generation European Centre for Medium-Range Weather Forecasts (ECMWF) reanalysis data  
153 available globally from 1940 to present (Hersbach et al., 2020). ERA5 combines modelled data and observations  
154 to create a complete and consistent global climate dataset using advanced data assimilation methods. ERA5  
155 provides improved precipitation representation such as the inclusion of tropical cyclones when compared to the  
156 ERA-Interim (He et al., 2020; Jiao et al., 2021). In addition, ERA5-Land, a subset of ERA5 focusing on land  
157 areas, delivers more detailed climate information at higher spatial resolution (0.1°) from 1950 to the present  
158 compared to ERA5 (Hersbach et al., 2020). Here, ERA5-Land (referred to as ERA5) is used to evaluate its  
159 performance for global hydrological modelling. The data is freely available from Copernicus Climate Data Store  
160 (<https://cds.climate.copernicus.eu/cdsapp#!dataset/reanalysis-era5-land?tab=overview>).

161 CHIRPS is a high-resolution (0.05°) quasi-global rainfall product primarily developed for monitoring droughts  
162 and global environmental changes (Funk et al., 2015). CHIRPS provides coupled gauge-satellite precipitation  
163 estimates with a 0.05° spatial resolution and long-period records. The product is developed by combining satellite-  
164 only Climate Hazards group Infrared Precipitation (CHIRP), Climate Hazards group Precipitation climatology  
165 (CHPclim), and data from ground stations. CHIRP and CHPclim were developed based on calibrated infrared  
166 cold cloud duration (CCD) precipitation estimates and ground station data from the Global Historical Climate  
167 Network (GHCN). The product is available at the Climate Hazards Group (<https://www.chc.ucsb.edu/data/chirps/>)  
168 on daily, 10-day, and monthly timescales from the 1981-near present. Due to its availability at high spatial and  
169 temporal resolution, CHIRPS is widely used in hydrological studies (Luo et al., 2019; Gebrechorkos et al., 2020;

170 Geleta and Deressa, 2021; Wang et al., 2021; Opere et al., 2022; Day and Howarth, 2019; Gebrechorkos et al.,  
171 2019) and modelling of hydrological extremes such as droughts and floods (Chen et al., 2020; Mianabadi et al.,  
172 2022; Peng et al., 2020).

173 MSWEP is a global high-resolution ( $0.1^\circ$ ) precipitation product developed by merging multiple datasets such as  
174 ground stations (~77,000), satellite-based rainfall estimates, and reanalysis data (Beck et al., 2019b). MSWEP  
175 was developed by merging station data, satellite datasets and reanalysis datasets (Beck et al., 2017b, 2019b).  
176 MSWEP has been widely used in regional and global scale hydrological studies such as for floods and droughts  
177 (Gu et al., 2023; Gebrechorkos et al., 2022b; Reis et al., 2022; Wu et al., 2018; Sun et al., 2022; Gebrechorkos et  
178 al., 2022c; Xiang et al., 2021; López López et al., 2017) and for developing high-resolution global scale  
179 hydrological extreme and climate datasets and regional drought monitoring (Gebrechorkos et al., 2023, 2022a; Li  
180 et al., 2022b). MSWEP is available from 1979-present at multiple timescales (e.g., 3 hourly) and can be accessed  
181 from the GloH2O website (<https://www.gloh2o.org/mswep/>).

182 TerraClimate (TERRA) is a high-resolution ( $0.04^\circ$ ) terrestrial monthly climate (e.g., precipitation and  
183 temperature) and climatic water-balance dataset available from 1958-2020 (Abatzoglou et al., 2018). TERRA was  
184 developed by combining high and coarse spatial resolution datasets such as WorldClim climatological normals  
185 and Climatic Research Unit gridded Time Series (CRU TS) and JRA-55, respectively. The data was evaluated  
186 against ground observation from the Historical Climate Network and exhibited better performance than the CRU-  
187 TS (Abatzoglou et al., 2018). The monthly climate and climatic water balance is available from the Climatology  
188 Lab website (<https://www.climatologylab.org/>).

189 CPCU is a gauge-based analysis of daily precipitation datasets available globally from 1979 to present at a spatial  
190 resolution of  $0.5^\circ$  (Chen et al., 2008). CPCU is the product of the CPC Unified Precipitation project at NOAA  
191 Climate Prediction Center. The product uses data from more than 30,000 (1979-2005) and 17,000 (2006-present)  
192 stations. The CPCU data is publicly available at the NOAA Physical Sciences Laboratory (PSL,  
193 [https://downloads.psl.noaa.gov/Datasets/cpc\\_global\\_precip/](https://downloads.psl.noaa.gov/Datasets/cpc_global_precip/)) and has been used for hydrological and climate  
194 studies (Beck et al., 2017a; Zhu et al., 2021; Hou et al., 2014).

195 The PERCCDR is a quasi-global (latitude from  $60^\circ\text{S}$  to  $60^\circ\text{N}$ ) dataset developed at the University of California  
196 (Sadeghi et al., 2021). PERCCDR provides precipitation estimates at high spatial ( $0.04^\circ$ ) and temporal (3-hourly)  
197 resolutions from 1983 to present. The dataset is developed using the rain rate output from the PERSIANN-CCS  
198 model, which uses GridSat-B1 IR and NOAA Climate Prediction Center (CPC-4km) IR data. Compared to other  
199 PERSIANN precipitation datasets, PERCCDR provides a realistic representation of precipitation extremes  
200 globally and shows better agreement with CPCU precipitation (Sadeghi et al., 2021). The PERCCDR has been  
201 used in hydrological studies (Salehi et al., 2022; Eini et al., 2022) and is freely available from the Center for  
202 Hydrometeorology and Remote Sensing (CHRS) Data Portal (<https://chrsdata.eng.uci.edu/>).

203 Table 1. The six precipitation datasets used in this study, their spatial and temporal resolution, spatial coverage  
204 and data sources.

Abbreviation	Full name	Spatial resolution and coverage	Temporal resolution	Temporal coverage	Data source	Reference
ERA5	ECMWF (European Centre for Medium-Range Weather Forecasts) Reanalysis V5	0.1°, global	Sub-daily	1979-present	Gauge and reanalysis	(Hersbach et al., 2020)
CHIRPS	Climate Hazards group Infrared Precipitation with Stations (CHIRPS) version 2.0	0.05°, quasi global (50°S-50°N)	Daily	1981-present	Gauge, satellite, and reanalysis	(Funk et al., 2015)
MSWEP	Multi-Source Weighted-Ensemble Precipitation (MSWEP) version 2.80	0.1°, global	Daily	1979-present	Gauge, satellite, and reanalysis	(Beck et al., 2019b)
TERRA	TerraClimate	0.042°, global	Monthly	1958-present	Gauge and reanalysis	(Abatzoglou et al., 2018)
CPCU	Climate Prediction Centre (CPC) Unified V1.0	0.5°, global	Daily	1979-present	Gauge only	(Chen et al., 2008)
PERCCDR	Precipitation Estimation from Remotely Sensed Information using Artificial Neural Networks-Cloud Classification System-Climate Data Record (PERSIANN-CCS-CDR)	0.04°, Quasi global (60°S-60°N)	Sub-daily	1983-present	Gauge and satellite	(Sadeghi et al., 2021)

## 205 2.2. WBMsed hydrological model

206 The WBMsed (Cohen et al., 2013, 2014) hydrological model is used to assess the performance of the different  
207 precipitation datasets for hydrological modelling globally. WBMsed is a global-scale hydrogeomorphic model,  
208 an extension of the WBMplus global hydrology model (Wisser et al., 2010), which is part of the FrAMES  
209 biogeochemical modelling framework (Wollheim et al., 2008). The WBMplus model is one of the first Global  
210 Hydrological Models (GHMs) applied to a global domain (Cohen et al., 2013; Grogan et al., 2022). The model  
211 represents the major hydrological cycle components of the land surface and tracks the balances and fluxes between

212 the atmosphere, surface water storages, vegetation, runoff, and groundwater (Grogan et al., 2022). The model  
213 includes hydrological infrastructure (e.g., dams), agricultural water requirements, and domestic and industrial  
214 water uses. A gridded river network connects grid cells, which allows the routing of fluxes downstream (e.g.,  
215 streamflow). The model requires several climate datasets as input in addition to precipitation, including  
216 temperature, humidity, air pressure, and wind speed (Table S1). Additional parameters such as field capacity,  
217 rooting depth, and riverbed slope are used to drive the model.

218 We use an identical model setup to that used by Cohen et al., (2022) with all input datasets as detailed in Cohen  
219 et al. (2013). Updates include daily ERA5 air temperature (Hersbach et al., 2020) re-gridded at 10 arc-minutes  
220 resolution, reservoir capacity from global reservoir and dam database (GRanD v1.3; Lehner et al., (2011)), and a  
221 6 arc-minute HydroSTN30 network derived from HydroSHEDS (Lehner et al., 2008) for flow network. In  
222 addition, we used each of our six input precipitation datasets, ERA5, CHIRPS, MSWEP, TERRA, CPCU, and  
223 PERCCDR in turn, keeping all other parameters and inputs the same. All the input precipitation datasets are  
224 bilinearly interpolated to the same spatial resolution of 0.1°. Even though WBMsed can disaggregate monthly  
225 time series into daily, TERRA (only available at monthly resolution, see Table 1) is evaluated on monthly and  
226 annual time scales, whilst all other datasets are evaluated at daily, monthly and annual time scales. WBMsed  
227 simulations were run at 0.1° (~11km at the equator) spatial and daily and monthly temporal resolutions. Several  
228 WBMsed streamflow validation analyses have been reported previously (e.g., Cohen et al., 2022; Dunn et al.,  
229 2019; Cohen et al., 2014, 2013; Moragoda and Cohen, 2020), which indicate that the model represents the long-  
230 term average observed streamflow globally. It is important to note that this study assesses the precipitation datasets  
231 without calibration of the WBMsed model for each precipitation dataset, which could theoretically improve their  
232 performance in replicating observed river discharge.

### 233 **2.3. Observed river discharge from ground stations**

234 Observed daily and monthly river discharge used to evaluate the hydrological model were obtained from the  
235 Global Runoff Data Centre (GRDC, 2023). The GRDC is an international data archive  
236 (<https://www.bafg.de/GRDC/>), which hosts data for over 10,000 hydrological stations. The number of stations  
237 with a length of record greater than 10 years during the evaluation period (1981-2019) are limited. Here, we  
238 consider stations with a minimum record length of 10 years, allowing for missing values within this period. Due  
239 to the spatial resolution of the input datasets and the model simulations (~11x11 km), we only consider stations  
240 with a catchment area of greater than 100 km<sup>2</sup>. Overall, 1825 suitable stations were identified with daily and  
241 monthly records, largely in North and South America, Europe and Australia, with very few stations in Africa and  
242 Asia (Figure 1).

### 243 **2.4. Evaluation metrics**

244 Several methods are used to assess the modelled discharge using the streamflow observations: the Pearson  
245 correlation coefficient (CC, Eq. 1), Kling-Gupta Efficiency (KGE, Eq. 2) (Gupta et al., 2009), Root-Mean-Square  
246 Error (RMSE, Eq.3) and Percentage of bias (Pbias, Eq.4). CC measures the linear relationship between observed  
247 discharge and simulated discharge, focusing primarily on the degree of association between the two datasets. It is

248 particularly useful for assessing the strength and direction of this relationship, highlighting how well the model  
 249 captures the variability in discharge (Moazami et al., 2013). KGE is a comprehensive metric that evaluates the  
 250 overall agreement between observed and simulated streamflow, considering similarities in variability, amplitude,  
 251 and timing. It provides an assessment of the model's ability to capture both the magnitude and temporal dynamics  
 252 of the observed discharge (Gupta et al., 2009). RMSE measures the average magnitude of the differences between  
 253 observed and simulated discharge, providing a measure of the overall goodness of fit. Moreover, the percentage  
 254 of bias is used to quantify the systematic overestimation or underestimation of discharge by the model compared  
 255 to observations (Moazami et al., 2013). A KGE value of 1.0 indicates a perfect match between the observed and  
 256 simulated discharge, whereas values lower than -0.41 show that the model is worse than using the mean of the  
 257 observed discharge as a predictor (Knoben et al., 2019). For spatial comparison, the RMSE is normalised by the  
 258 standard deviation of the observed data (NRMSE; Eq. 5).

$$259 \quad CC = \frac{\sum_{i=1}^N (M_i - \bar{M}) * (O_i - \bar{O})}{\sqrt{\sum_{i=1}^N (M_i - \bar{M})^2} * \sqrt{\sum_{i=1}^N (O_i - \bar{O})^2}} \quad (1)$$

$$260 \quad KGE = 1 - \sqrt{(r - 1)^2 + (\alpha - 1)^2 + (\beta - 1)^2} \quad (2)$$

$$261 \quad RMSE = \sqrt{\frac{\sum_{i=1}^N (O_i - M_i)^2}{N}} \quad (3)$$

$$262 \quad Pbias = \frac{\sum_{i=1}^N (M_i - O_i)}{\sum_{i=1}^N O_i} * 100 \quad (4)$$

$$263 \quad NRMSE = \frac{RMSE}{SD} * 100 \quad (5)$$

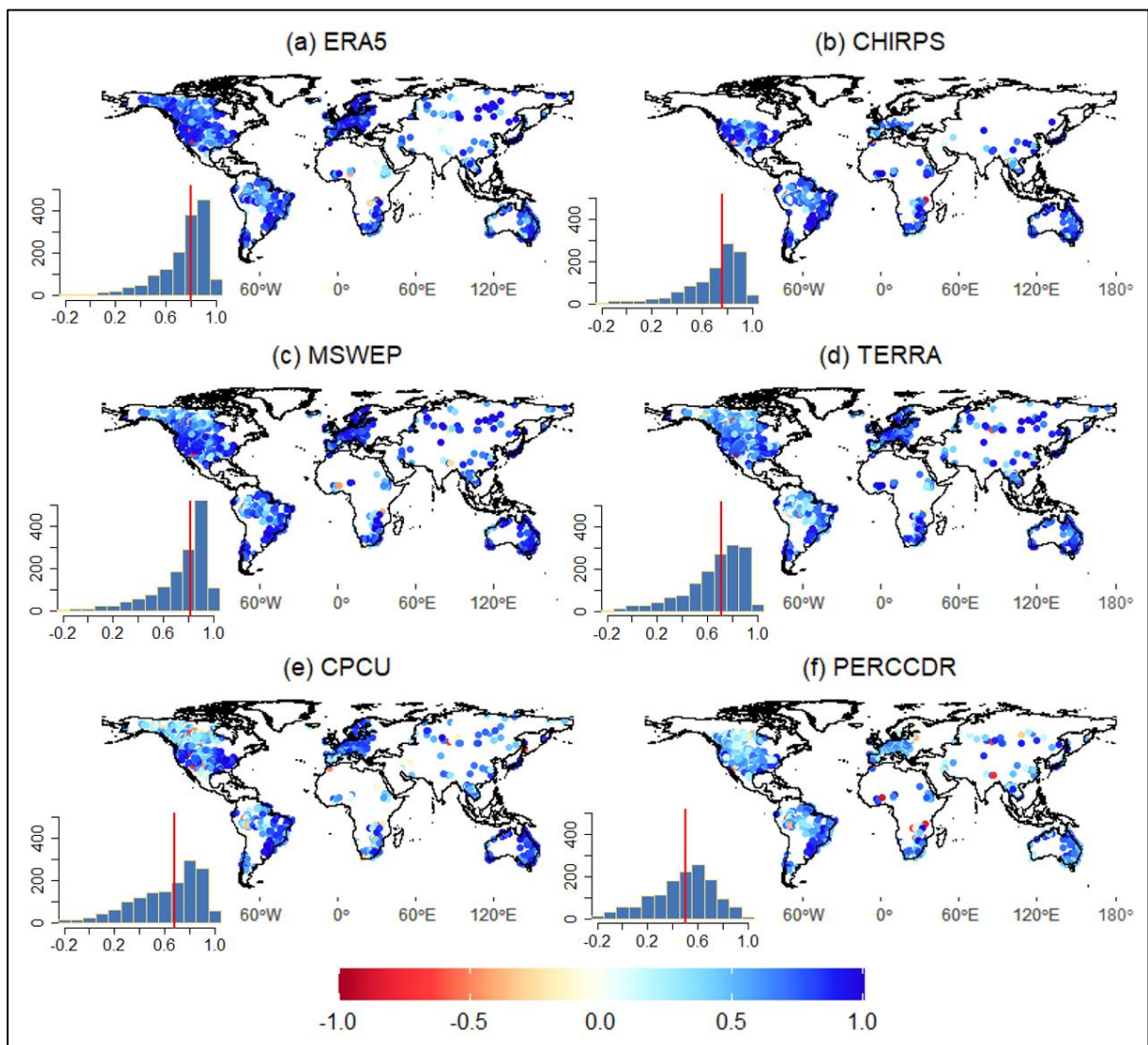
264 where  $r$  is the linear correlation between observed ( $O$ ) and modelled ( $M$ ) discharge and  $\alpha$  and  $\beta$  are the variability  
 265 and bias ratios, respectively. The NRMSE and SD are the normalised RMSE and standard deviation, respectively.  
 266 To assess the performance of the precipitation datasets for representing daily hydrological extremes, the 90<sup>th</sup> and  
 267 10<sup>th</sup> percentile are used, which indicates high and low flows, respectively. To derive high and low flow thresholds  
 268 from a daily flow time series, the data is first arranged in ascending order. The 90<sup>th</sup> percentile (Q10) is determined  
 269 as the flow value below which 90% of the daily flows occur, representing high-flow conditions. Conversely, the  
 270 10<sup>th</sup> percentile (Q90) represents the flow value below which just 10% of the daily flows lie, indicating low-flow  
 271 conditions.

## 272 **3. Results**

### 273 **3.1. Performance of the six precipitation datasets for annual discharge prediction**

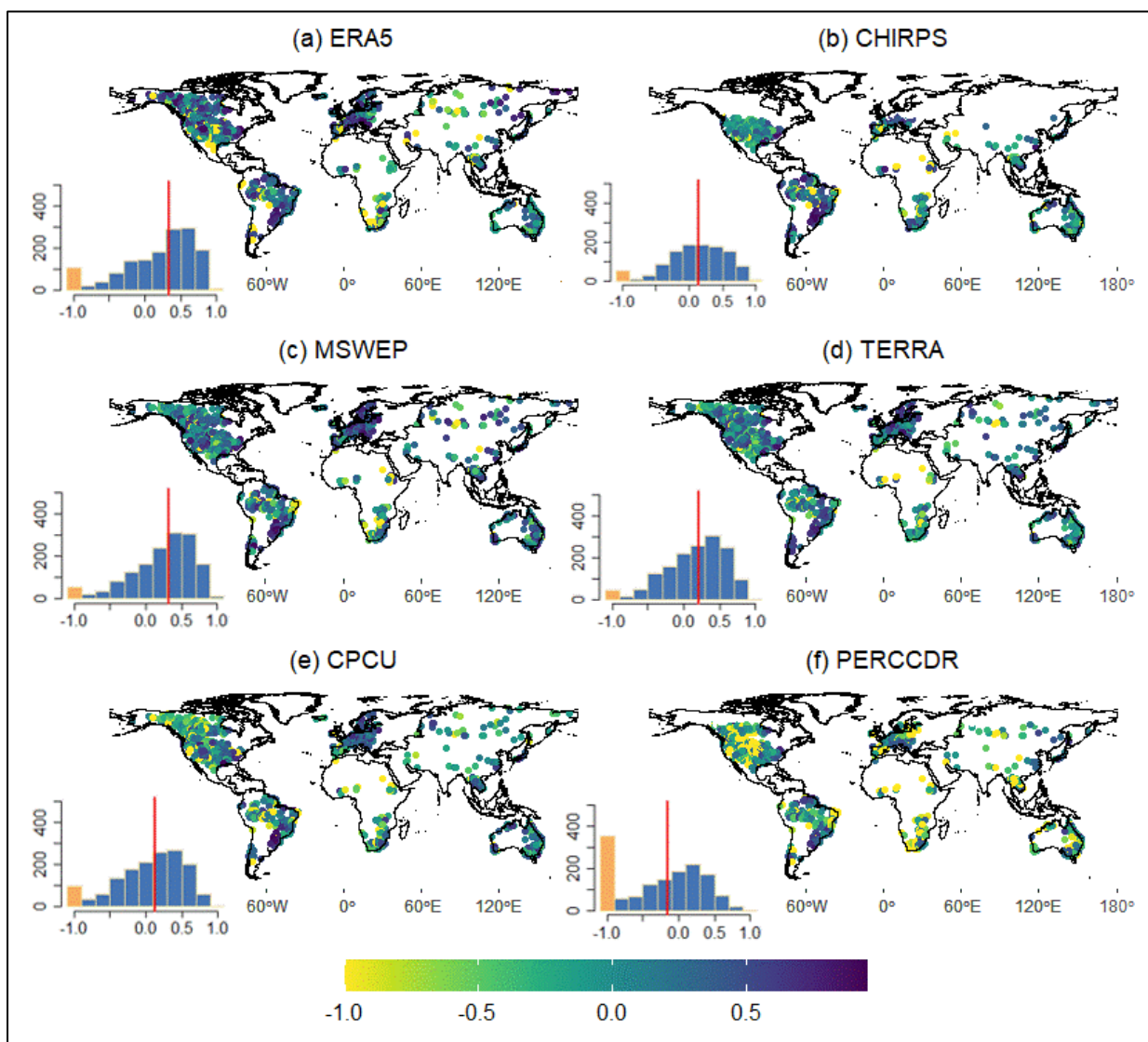
274 The temporal correlation coefficient (CC) between the observed and simulated annual discharge based on the six  
 275 precipitation datasets is summarised in Figure 1. Most of the datasets, particularly ERA5, MSWEP, and CHIRPS,  
 276 showed a high CC in basins of Europe (e.g., Danube basin), South America (e.g., Rio de la Plata-Parana), North  
 277 America and Australia (e.g., Murray-Darling). MSWEP and ERA5 showed the highest CC for 34% and 32% of  
 278 the stations, respectively, followed by CPCU and CHIRPS. The TERRA and PERCCDR were the least well-

279 performing datasets with lower CC overall, and a higher CC than other datasets for less than 9% of stations. The  
 280 median CC of MSWEP and ERA5 is 0.82 and 0.8, respectively. MSWEP and TERRA showed lower Pbias and  
 281 NRMSE compared to the other datasets (Figures S1 and S2). ERA5 and PERCCDR showed a high NRMSE (up  
 282 to 247%) and Pbias (up to 99%) for more than 46% of stations. Similar to the CC, ERA5 and MSWEP  
 283 outperformed the other datasets for KGE, with higher values for 32% and 27% of stations, respectively. The  
 284 performance of MSWEP and ERA5 is higher in basins of Europe, South America, and Australia compared to Asia  
 285 and Africa. The median KGE values of ERA5 and MSWEP are 0.33 and 0.32, respectively (Figure 2). The  
 286 PERCCDR and CPU demonstrate high KGE only in about 9% of the stations, with median values of 0.10 and  
 287 0.13, respectively. Based on the annual CC and KGE, there is no single precipitation dataset that is best  
 288 everywhere, and even the least well-performing dataset overall shows better performance in some stations (Figure  
 289 3). Figure 3 summarizes the spatial representation of precipitation dataset performance, highlighting the individual  
 290 datasets exhibiting the highest CC and KGE values at each observation point.



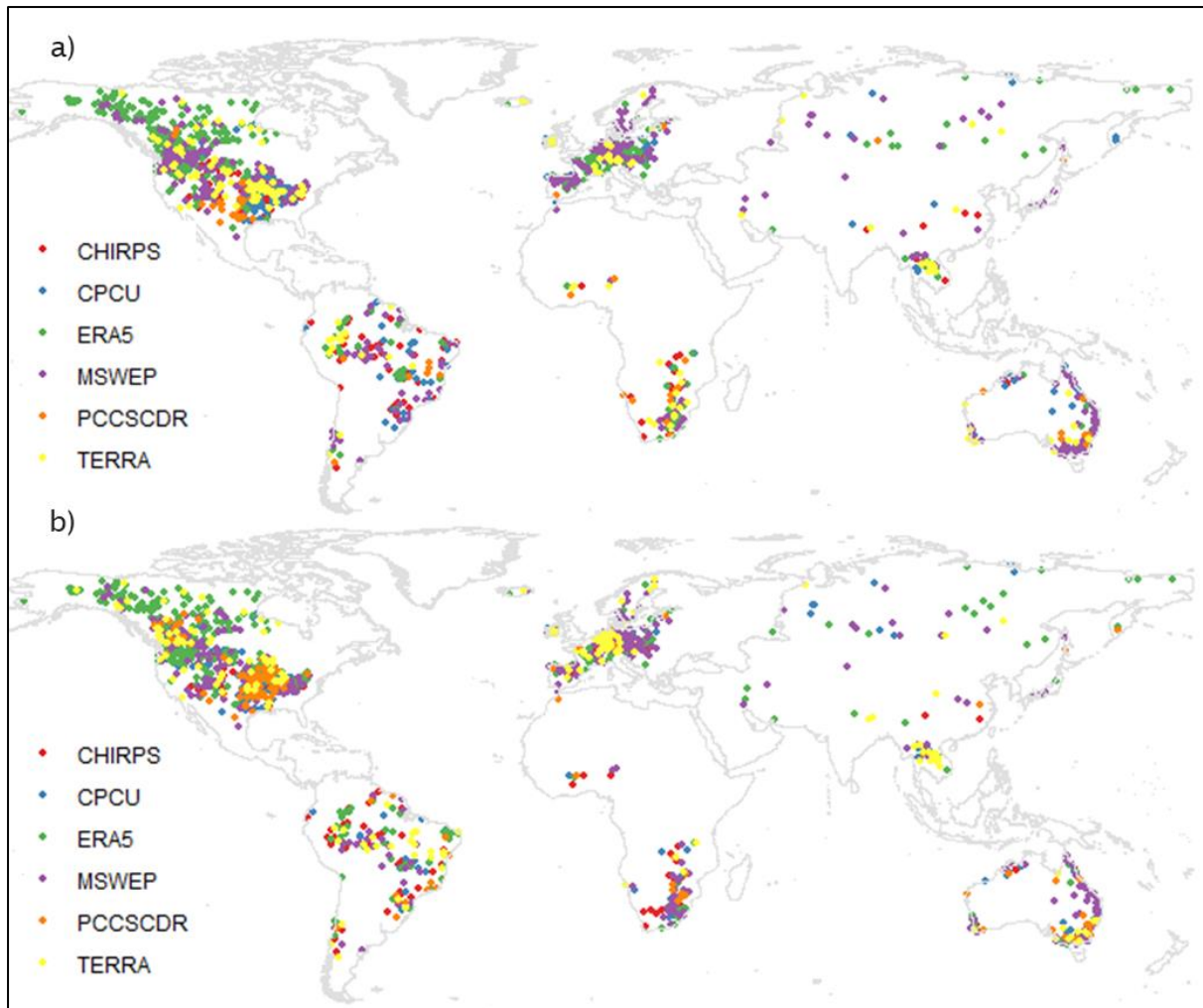
291

292 **Figure 1: Correlation (CC) between annual observed and modelled streamflow data using a) ERA5, b) CHIRPS, c)**  
 293 **MSWEP, d) TERRA, e) CPCU and f) PERCCDR precipitation datasets. The inset histograms show the frequency**  
 294 **distribution (y-axis) of the annual CC (x-axis), with the red vertical line indicating the median value.**



296

297 **Figure 2: KGE between observed and modelled annual streamflow based on a) ERA5, b) CHIRPS, c) MSWEP, d)**  
 298 **TERRA, e) CPCU, and f) PERCCDR precipitation datasets. KGE values below -0.41 indicate bad model performance**  
 299 **than using observed discharge mean as a predictor. The inset histograms show the frequency distribution (y-axis) of**  
 300 **the annual KGE (x-axis). KGE values lower than -1 are highlighted in orange. The red vertical line indicates the median**  
 301 **value.**

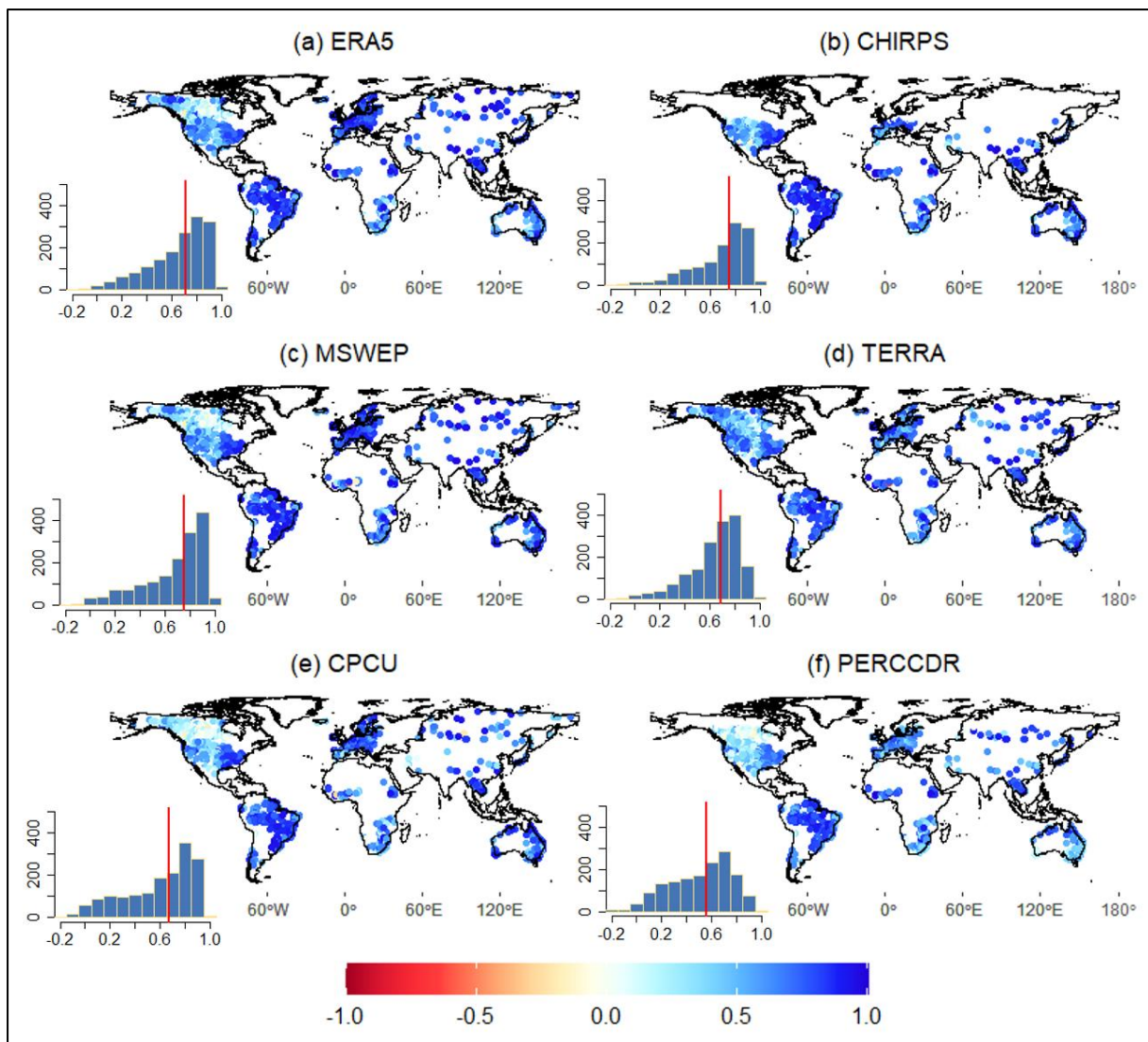


302

303 **Figure 3: The best performing precipitation dataset (ERA5, CHIRPS, MSWEP, TERRA, CPCU, and PERCCDR) at**  
 304 **each of the observed discharge stations based on annual CC (a) and KGE (b).**

305 **3.2. Performance of the six precipitation datasets for monthly discharge predictions**

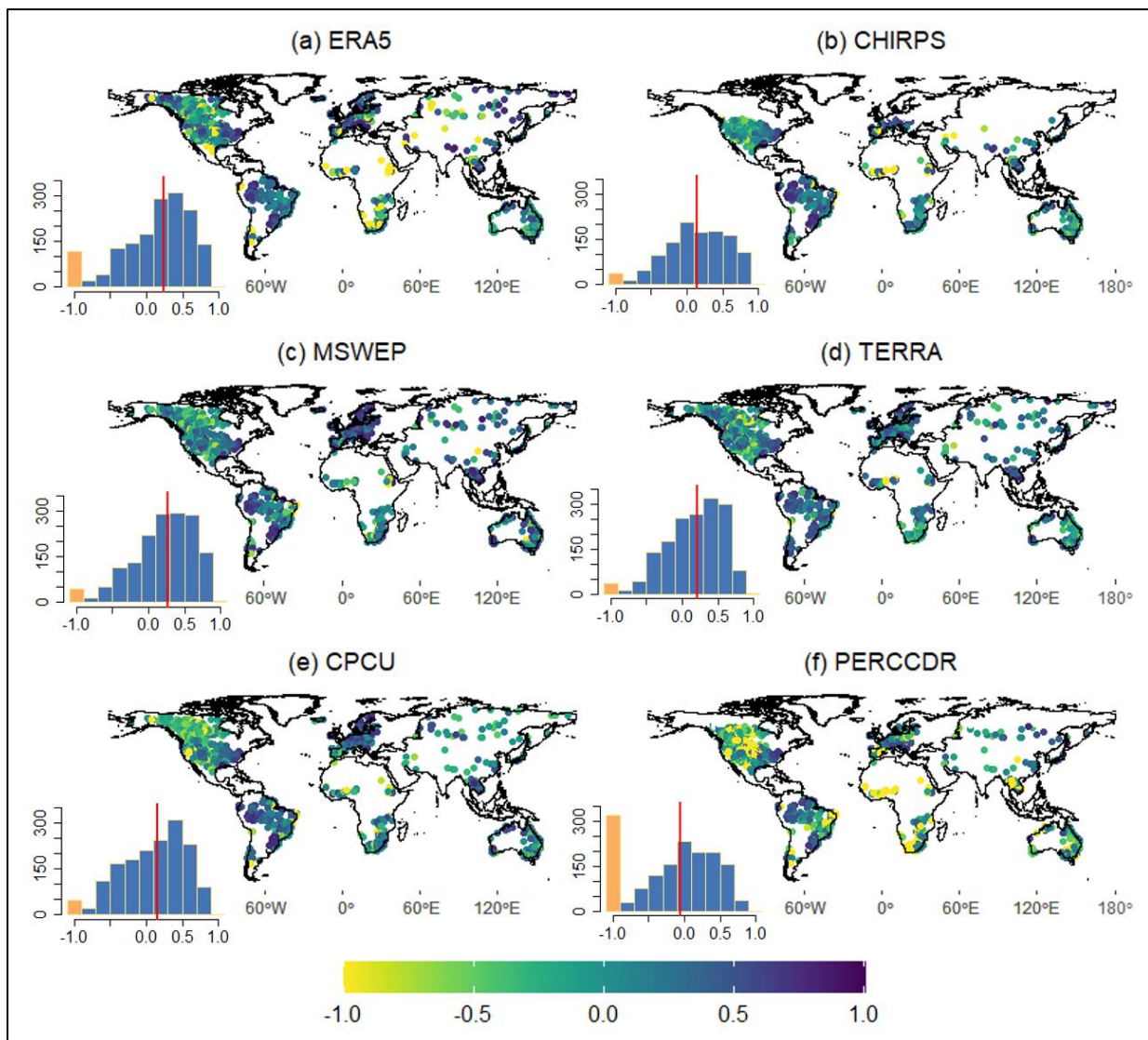
306 The six precipitation datasets consistently demonstrate high CC at a monthly scale in large parts of the world,  
 307 except in some rivers of Canada and Australia (Figure 4). The monthly CC, similar to the annual CC, shows a  
 308 relatively better performance of MSWEP with a median CC of 0.76. TERRA is the second-best with a median  
 309 CC of 0.69. MSWEP and TERRA show a higher CC than other datasets in 35% and 28% of the stations,  
 310 respectively. ERA5 and CHIRPS are ranked as the third and fourth datasets with a median CC of 0.71 and 0.75,  
 311 respectively. CPCU and PERCCDR are the least well-performing datasets, which only show the highest CC in  
 312 less than 6% of the stations with a median CC of 0.67 and 0.56, respectively.



313

314 **Figure 4: Correlation (CC) between monthly observed and modelled streamflow data based on a) ERA5, b) CHIRPS,**  
 315 **c) MSWEP, d) TERRA, e) CPCU and f) PERCCDR precipitation datasets. The inset histograms show the frequency**  
 316 **distribution (y-axis) of the monthly CC (x-axis), with the red vertical line indicating the median value.**

317 The monthly KGE also indicates the better performance of ERA5 and MSWEP for 26% and 24% of stations,  
 318 respectively (Figure 5). MSWEP showed a lower Pbias and NRMSE than all datasets, except in 5% of the stations  
 319 (Figures S3 and S4). Compared to MSWEP, ERA5 showed a larger Pbias and NRMSE in 15% and 19% of the  
 320 stations. TERRA, a third-best performing dataset based on KGE (18% of stations), shows a lower monthly Pbias  
 321 and RMSE in 85% of the stations compared to CHIRPS, ERA5, and PERCCDR. Compared to all datasets, the  
 322 PERCCDR showed a higher NRMSE and Pbias in 55% and 28% of the stations, respectively.

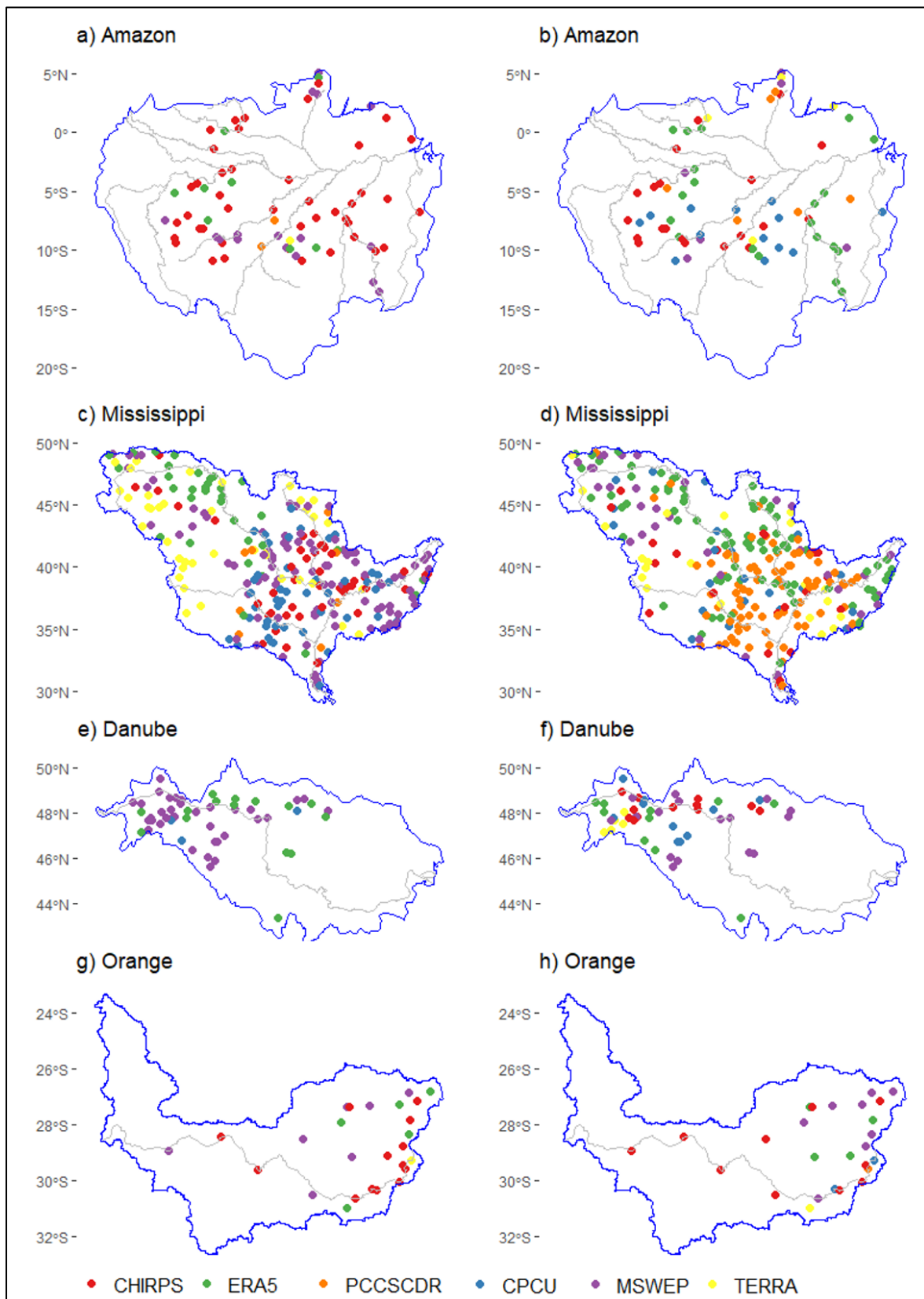


323

324 **Figure 5: Monthly KGE values between observed and modelled streamflow based on a) ERA5, b) CHIRPS, c) MSWEP,**  
 325 **d) TERRA, e) CPCU and f) PERCCDR precipitation datasets. KGE values below -0.41 indicate model performance**  
 326 **that is worse than using the observed discharge mean as a predictor. The inset histograms show the frequency**  
 327 **distribution (y-axis) of the monthly KGE (x-axis). KGE values lower than -1 are highlighted in orange, with the red**  
 328 **vertical line indicating the median value.**

329 The spatial representation of the six precipitation datasets in the Amazon, Mississippi, Danube, and Orange River  
 330 basins is summarised in Figure 6, highlighting the individual datasets exhibiting the highest CC and KGE values  
 331 at each hydrological station. In the Amazon basin, ERA5 (31%) and CHIRPS (29%) emerge as the top performers,  
 332 while PERCCDR (8%) and TERRA (5%) rank lower among the precipitation datasets. In the Mississippi basin,  
 333 MSWEP leads with higher CC in 37% of stations, and ERA5 exhibits higher KGE in 31% of the stations. Notably,  
 334 PCCSCDR displays higher KGE values than MSWEP, TERRA, CHIRPS, and CPCU in 30% of Mississippi  
 335 stations. Across the Danube basin, MSWEP outperforms the other products with a higher CC in 66% of stations  
 336 and KGE in 30% of the stations, while TERRA and CPCU are the least performing products. Furthermore,  
 337 CHIRPS, in 52% of stations based on CC and 37% based on KGE, outperformed other datasets in the Orange

338 River basin. In Orange, MSWEP ranks second with higher KGE and CC in about 27% of stations, while TERRA  
 339 and PCCSCDR are the least performing datasets.



340

341 **Figure 6: Performance of precipitation datasets (ERA5, CHIRPS, MSWEP, TERRA, CPCU, and PERCCDR) at**  
 342 **discharge stations in a) Amazon, c) Mississippi, e) Danube, and g) Orange river basins based on their monthly CC.**  
 343 **Performance of the datasets based on KGE for the Amazon, Mississippi, Danube, and Orange River Basins is illustrated**  
 344 **in figures b, d, f, and h, respectively.**

345 Table 2 summarises the monthly KGE between observed and modelled streamflow, based on the six precipitation  
 346 datasets, for selected locations in basins of Africa (Niger, Lokoja), Asia (Mekong, Khong-Chiam), South America  
 347 (Amazon, Missao-Icana), North America (Mississippi, Savannah), Australia (North East Coast, Mirani-Weir),  
 348 and Europe (Danube, Dunaalmas). The basins were chosen to represent a diverse range of climatic regions and  
 349 drainage areas where there was availability of a long time series of observed data (Figure S5). In Niger, the  
 350 observed monthly flow and variability at Lokoja station are very well reproduced by CHIRPS and TERRA with  
 351 a CC of 0.88 and 0.85, respectively (Figure S5a). Even though CPCU showed a lower CC (0.64) at Lokoja, it  
 352 showed a higher KGE (0.62) and lower Pbias (0.4%) compared to the other products. At Lokoja, PERCCDR is  
 353 the least well-performing dataset with the highest RMSE and Pbias and lowest KGE. The monthly variability at  
 354 the Khong-Chiam station is reproduced by all the precipitation products with a CC of greater than 0.91, with  
 355 MSWEP and TERRA showing the lowest bias and RMSE. ERA5 and CHIRPS performed well at station Missao-  
 356 Icana in the Amazon with a CC of 0.9 and RMSE of about 610 m3/s. For stations Savannah, Mirani-Weir, and  
 357 Dunaalmas, MSWEP is the best product with higher CC (> 0.72) and KGE (> 0.62) and lower Pbias and RMSE  
 358 (Figures S5d - S5f).

359 Table 2. KGE of monthly predictions for selected stations in basins of Africa (Niger), Asia (Mekong), South  
 360 America (Amazon), North America (Mississippi), Australia (North East Coast), and Europe (Danube).

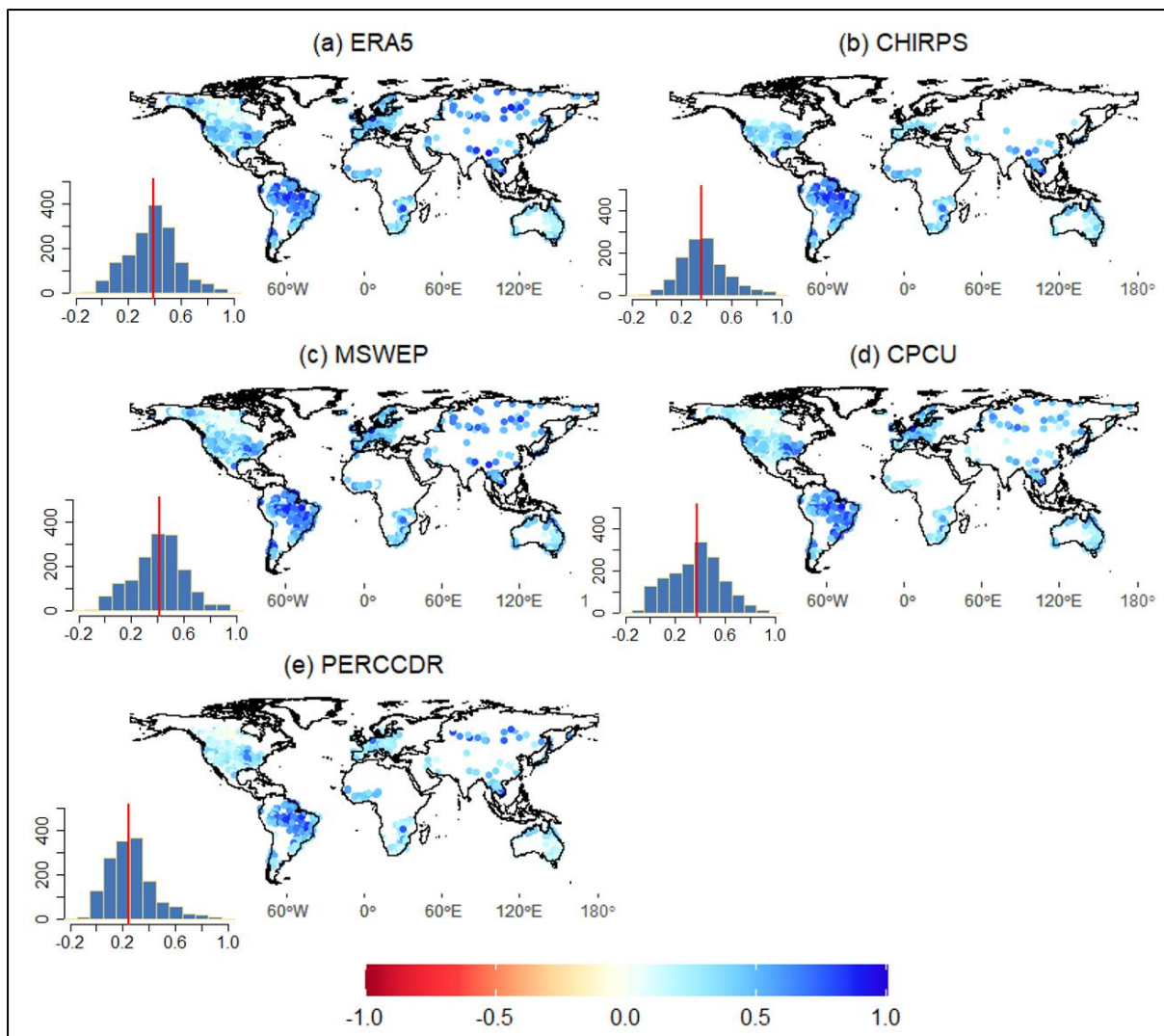
Basin	Stations name	Longitude	Latitude	Catchment area (km <sup>2</sup> )	ERA5	CHIRPS	MSWEP	TERRA	CPCU	PERCCDR
Niger	Lokoja	6.8	7.8	1670000	0.21	-0.1	0.60	0.34	0.62	-0.99
Mekong	Khong Chiam	105.5	15.3	419000	0.13	0.56	0.70	0.91	0.70	-0.04
Amazon	Missao Icana	-67.6	1.1	22282	0.71	0.78	0.73	0.72	0.61	0.65
Mississippi	Savannah	-88.3	35.2	85833	0.59	0.65	0.67	0.66	0.53	0.66
North East Coast	Mirani-Weir	148.8	-21.2	1211	-0.1	0.38	0.62	0.44	0.46	-0.05
Danube	Dunaalmas	18.3	47.7	171720	0.34	0.73	0.78	0.52	0.71	-0.49

361

362

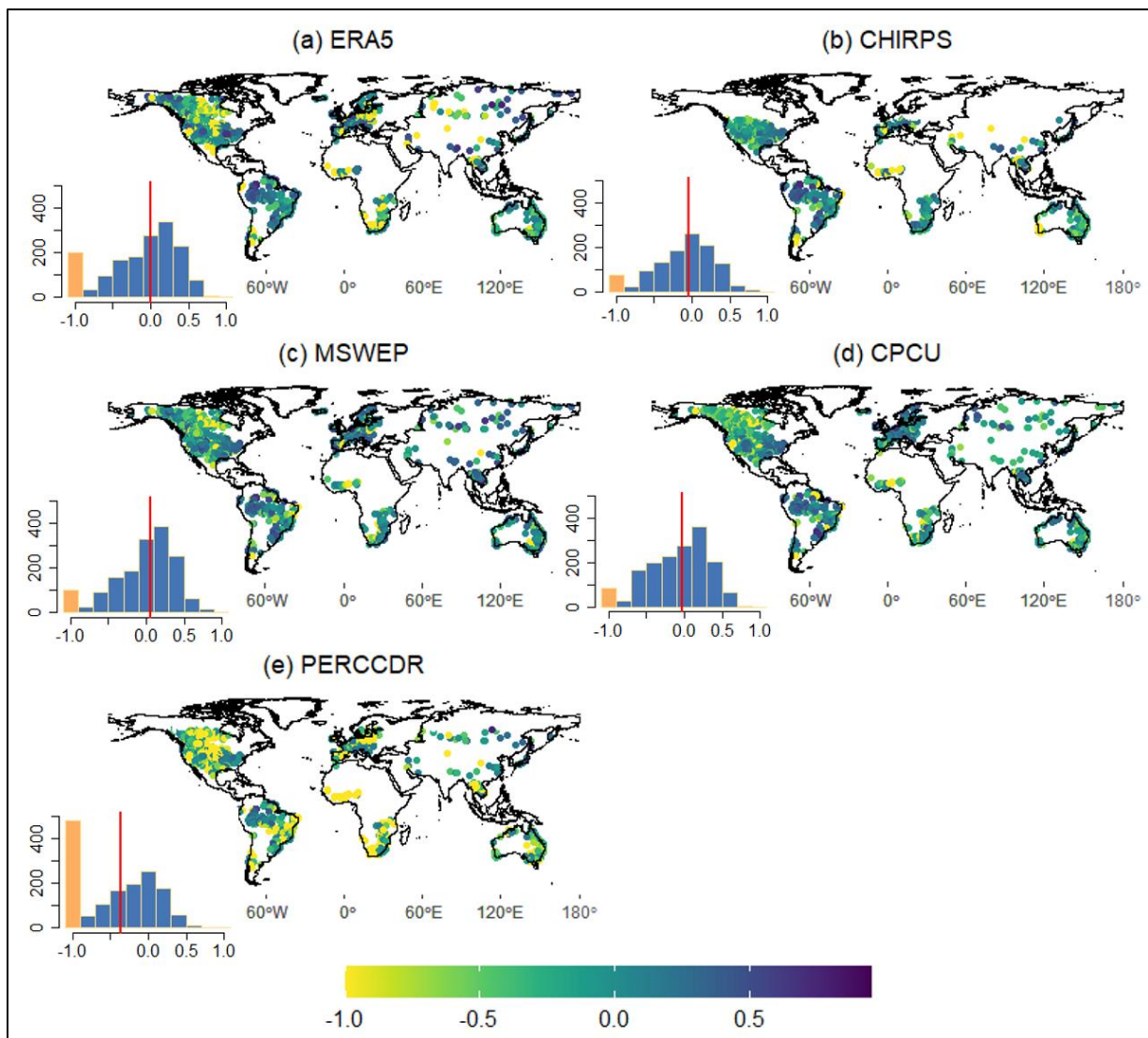
363 **3.3. Performance of the precipitation datasets for daily and daily extreme discharge predictions**

364 Based on the daily evaluation, MSWEP followed by ERA5 show a higher CC in more than 50% of the stations  
365 with median values of 0.41 and 0.39, respectively (Figure 7). ERA5 and MSWEP performed well in 31% and  
366 31% of the stations with high KGE values (Figure 8). Similar to the monthly evaluation, PERCCDR shows poorer  
367 performance (lower CC and KGE, higher biases and errors) in almost 95% of the stations. Even though ERA5  
368 showed a higher CC and KGE in 30% of the stations it shows a higher NRMSE (up to 250%) and Pbias (up to  
369 100%) in 20% and 30% of the stations (Figures S6 and S7). Overall, MSWEP and CHIRPS showed lower NRMSE  
370 and Pbias compared to the other products. The CC and KGE of all the products (except CHIRPS) are lower in  
371 North America compared to stations in South America, Europe, and Australia. The spatial representation of  
372 precipitation dataset performance, highlighting the individual datasets exhibiting the highest daily CC and KGE  
373 values at each observation point, is provided in Figure S9. Additionally, Figure S10 depicts the spatial  
374 representation of each precipitation dataset for the Amazon, Mississippi, Danube, and Orange River Basins. In  
375 the Mississippi basin, ERA5 exhibited the highest KGE and CC values, followed by MSWEP and CPCU (Figure  
376 S10). In the Amazon basin, ERA5 and CHIRPS displayed the highest KGE and CC values compared to the other  
377 datasets. For the Danube basin, CPCU followed by MSWEP emerged as the best precipitation product relative to  
378 ERA5, PCCSCDR, and CHIRPS. In the Orange River Basin, MSWEP based on CC and CHIRPS based on KGE  
379 were the top-performing products, while PCCSCDR performed the least.



380

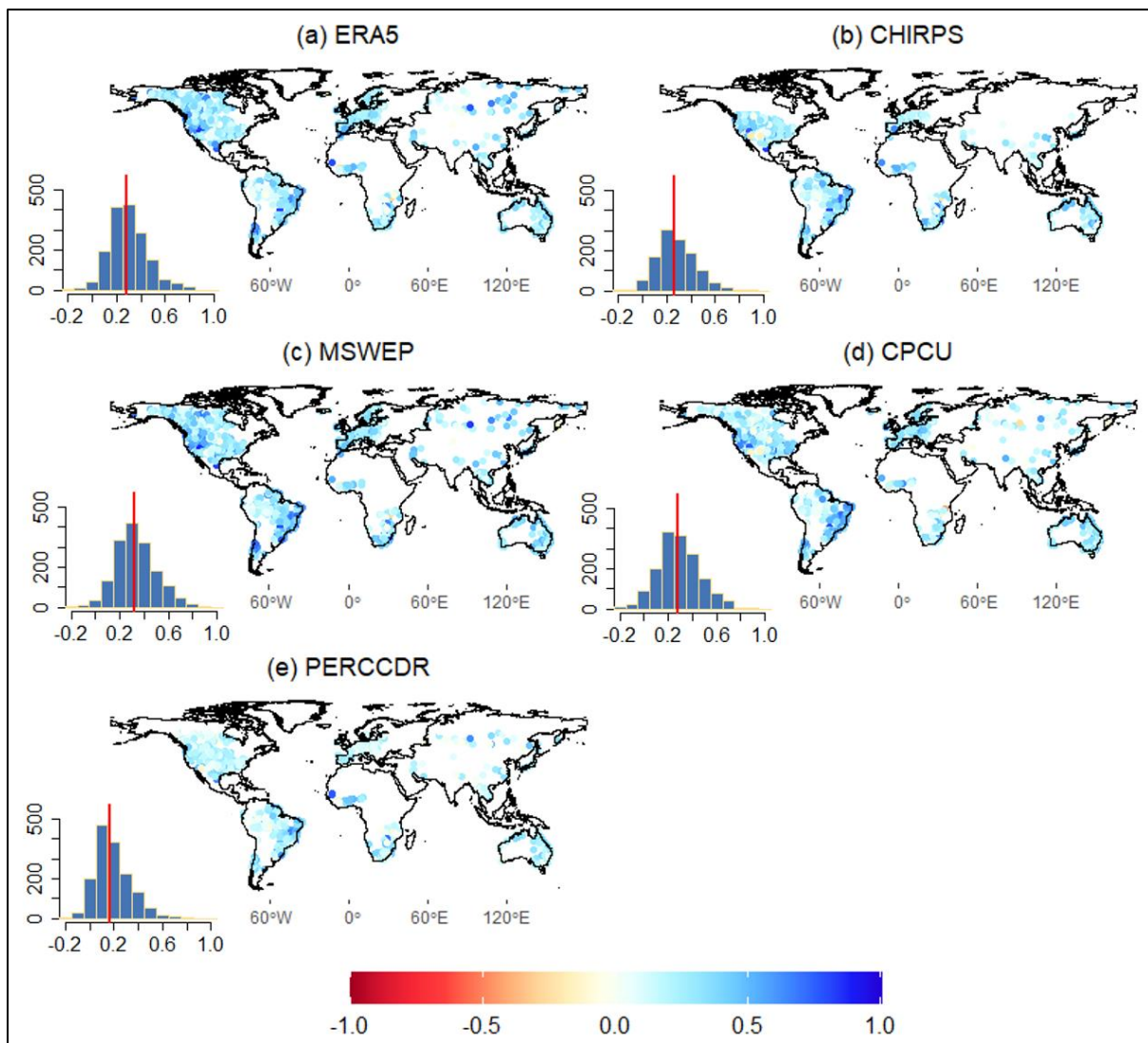
381 **Figure 7: Correlation (CC) between daily observed and modelled streamflow data using a) ERA5, b) CHIRPS, c)**  
 382 **MSWEP, d) CPCU and e) PERCCDR precipitation datasets. The inset histograms show the frequency distribution (y-**  
 383 **axis) of the daily CC (x-axis), with the red vertical line indicating the median value.**



384

385 **Figure 8: Daily KGE values between observed and modelled streamflow based on a) ERA5, b) CHIRPS, c) MSWEP,**  
 386 **d) CPCU, and e) PERCCDR precipitation datasets. KGE values below -0.41 indicate bad model performance than**  
 387 **using observed discharge mean as a predictor. The inset histograms show the frequency distribution (y-axis) of the**  
 388 **daily KGE (y-axis). KGE values lower than -1 are highlighted in orange, with the red vertical line indicating the median**  
 389 **value.**

390 The performance of the daily precipitation products is also assessed for daily extremes in terms of the Q10 and  
 391 Q90 values. Based on the CC, MSWEP is the best-performing dataset for Q10 (Figure 9) and Q90 (Figure S8).  
 392 For Q10, MSWEP and CPCU exhibited a higher CC than other datasets at 38% and 32% of the stations,  
 393 respectively. Similarly, for Q90, MSWEP and ERA demonstrated a higher CC compared to other datasets at 35%  
 394 and 30% of the stations. The median CC for Q10 (Q90) is 0.32 (0.41), 0.28 (0.36), 0.27 (0.35), 0.26 (0.38), and  
 395 0.16 (0.23) for MSWEP, CPCU, CHIRPS, ERA5, CHIRPS, and PERCCDR, respectively. Similar to the annual,  
 396 monthly and daily evaluations, PERCCDR showed poor performance for the two extremes (Q90 and Q10).  
 397 Overall, the performance of the datasets is lower for extremes compared to the annual, monthly and daily scales.



398

399 **Figure 9: Correlation (CC) between observed and modelled daily extremes (Q10, high flow) streamflow data a) ERA5,**  
 400 **b) CHIRPS, c) MSWEP, d) CPCU and e) PERCCDR precipitation datasets. The inset histograms show the frequency**  
 401 **distribution (y-axis) of the daily Q10 CC (x-axis), with the red vertical line indicating the median value.**

#### 402 **4. Discussion and Conclusion**

403 Based on the evaluation at annual, monthly and daily time scales and analysis of daily extremes, no single  
 404 precipitation dataset consistently exhibits high accuracy across all geographical regions, nor does one consistently  
 405 outperform the other datasets. This finding is in agreement with previous studies (Beck et al., 2017a; Dembélé et  
 406 al., 2020). A similar pattern of varied performance (e.g., lower in Africa and the central United States and better  
 407 in Europe) by different global hydrological models and precipitation datasets has been presented (Beck et al.,  
 408 2017a; Lin et al., 2019; Harrigan et al., 2020). In addition to the uncertainty in the precipitation datasets, the poorer  
 409 performance in some regions presented in this and previous studies (Beck et al., 2017a; Lin et al., 2019; Harrigan  
 410 et al., 2020) can be exacerbated by the lack of representation in the hydrological models of anthropogenic  
 411 influences, such as for agriculture, irrigation, water supply, and energy production.

412 Comparably, MSWEP and ERA5 consistently exhibited higher CC and KGE values at over 50% of the stations  
413 across annual, monthly, and daily time scales. According to Gu et al. (2023), satellite- and reanalysis-based  
414 precipitation datasets, such as MSWEP and ERA5, can provide satisfactory performance for simulating discharge  
415 globally. The higher performance of MSWEP indicates the advantage of incorporating a large number of daily  
416 observations from field-based meteorological stations, in addition to a large set of satellite and reanalysis datasets  
417 (Beck et al., 2017a, 2019a). Other studies have also shown the good performance of MSWEP for hydrological  
418 modelling in different parts of the world (Beck et al., 2017a; Lakew, 2020; Li et al., 2022a; Reis et al., 2022; Gu  
419 et al., 2023; López López et al., 2017; Satgé et al., 2019; Ibrahim et al., 2022). For example, Satgé et al. (2019)  
420 evaluated 12 satellite-based precipitation estimates such as MSWEP, CHIRPS and PERSIANN-CDR in South  
421 America (Lake Titicaca region) and found MSWEP was the best precipitation dataset for realistic simulation of  
422 river discharge. MSWEP was also found to be the most reliable precipitation dataset compared to multiple datasets  
423 such as CHIRPS and CMORPH for hydrological and climate studies in basins of Eastern China (Shaowei et al.,  
424 2022; Wu et al., 2018).

425 Even though ERA5 showed a higher KGE and CC than MSWEP, CHIRPS and TERRA in about 32% of the  
426 stations it showed a higher error and biases. Previous studies have revealed bias and errors in ERA5 precipitation  
427 (Lavers et al., 2021; Bechtold et al., 2020; AL-Falahi et al., 2020; Jiang et al., 2023; Lavers et al., 2022), which  
428 leads to propagated errors and bias in hydrological modelling outputs. Harrigan et al. (2020) also reported large  
429 biases in ERA5-driven hydrological simulations in the Central United States, South America (e.g., Brazil), and  
430 Africa. According to Lavers et al. (2022), ERA5 precipitation is more reliable in extratropical areas compared to  
431 tropical areas. Despite CPCU being a gauge-based precipitation dataset, it did not show as good performance as  
432 MSWEP and ERA5 on annual, monthly, and daily timescales. In addition to the lower KGE and CC, CPCU  
433 showed higher bias and error, particularly on annual and monthly time scales. The bias and errors in CPCU can  
434 be due to the coarse resolution (0.5°) and the limited number of stations used to develop the datasets, particularly  
435 in Africa and South America. According to Beck et al. (2017a), CPCU can be used in large river basins with dense  
436 meteorological stations but can be disadvantageous in Africa and South America. This highlights the need to  
437 expand and maintain the meteorological stations in these regions, but also the need to draw from satellite and  
438 model data sources. The PERSIANN-CDR is the least-performing product with lower KGE and higher errors and  
439 biases, which has been highlighted elsewhere in terms of its inability to represent precipitation extremes (Miao et  
440 al., 2015; Solakian et al., 2020).

441 The precipitation datasets show limited skill overall in reproducing daily extremes (high and low flows), relative  
442 to the annual and monthly time scales. MSWEP and CPCU have shown a high CC in about 38% of the stations.  
443 This is consistent with the findings of Tang et al., (2019) for the Mekong River Basin. CHIRPS and PERSIANN-  
444 CDR are the least skilful in capturing extremes with a very low CC and large positive and negative biases (Araujo  
445 Palharini et al., 2021). For instance, numerous precipitation products have been observed to both underestimate  
446 and overestimate low and high precipitation values in Brazil (Palharini et al., 2020), consequently resulting in  
447 corresponding underestimations and overestimations of low and high streamflows. In general, several studies have  
448 concluded that precipitation datasets exhibit a substantial disparity in daily extreme precipitation events (e.g.,  
449 Araujo Palharini et al., 2021; Jiang et al., 2019; Huang et al., 2022), which can be attributed to factors such as  
450 inaccuracies in satellite sensors, retrieval algorithms, temporal sampling, and satellite-observation merging and

451 bias correction procedures used, particularly in gauge-limited regions (Miao et al., 2015; El Kenawy et al., 2015;  
452 Shen et al., 2010; Jiang et al., 2019). In addition to the uncertainty of the precipitation datasets, the limited  
453 availability of hydrological observations limits the ability to assess these datasets globally, especially for extreme  
454 flood and drought events (Brunner et al., 2021).

455 Whilst the WBMsed model has been shown to perform well in predicting mean flows when compared to historical  
456 observations, for example Cohen et al. (2022) report an  $R^2$  of 0.99 in 30-year average prediction against USGS  
457 gauge data and global river datasets, it is important to acknowledge the uncertainties and limitations in the model  
458 parameterisation and initial conditions, including the role of anthropogenic impacts, which are greatly simplified  
459 in WBMsed. Many of the uncertainties in the precipitation input data, such as those derived from satellite-based  
460 precipitation datasets, including retrieval errors, can propagate through the hydrological model, potentially  
461 affecting the accuracy of simulated discharge. Globally calibrated model parameters may introduce further  
462 uncertainty, particularly in regions with limited observational data coverage. Due to the limited availability of  
463 observed discharge in Africa and Asia, evaluation predominantly focuses on North and South America and  
464 Europe. Hence, further evaluation in Africa and Asia could be essential to enhance the robustness of global  
465 hydrological models.

466 Overall, the evaluation presented in this paper underlines the importance of selecting high-quality precipitation  
467 datasets to drive hydrological models. Since no single precipitation dataset was found to be adequately accurate  
468 everywhere, across different temporal scales, this study can help identify the best precipitation products for any  
469 basin or region under consideration. Based on our results, MSWEP is the best overall choice but there are regions  
470 where ERA5, CHIRPS and CPCU were better overall. All the precipitation datasets, particularly ERA5 and  
471 PERCCDR, require bias correction before being used to drive hydrological models in regions like North America,  
472 Asia, Africa, and Australia. For data-scarce regions such as Africa and Asia, it is difficult to recommend a  
473 precipitation dataset due to the limited number of hydrological stations used for validation in this study. Finally,  
474 improving the precipitation datasets by adding more ground observations, for example, and by better representing  
475 anthropogenic drivers in hydrological models has the potential of considerably improving global and regional  
476 hydrological predictions.

#### 477 **Data availability**

478 The selected precipitation datasets used in this study are openly accessible to the public. ERA5 is freely available  
479 from the Copernicus Climate Data Store (CDS; <https://cds.climate.copernicus.eu/cdsapp#!/dataset/reanalysis-era5-land?tab=overview>). CHIRPS can be obtained from the Climate Hazards Group (CHG; <https://www.chc.ucsb.edu/data/chirps/>). Access to the MSWEP precipitation dataset is provided through the  
481 GloH2O website (<https://www.gloh2o.org/mswep/>). TERRA is accessible from the Climatology Lab website  
482 (<https://www.climatologylab.org/>). CPCU is publicly available through the NOAA Physical Sciences Laboratory  
483 (PSL; [https://downloads.psl.noaa.gov/Datasets/cpc\\_global\\_precip/](https://downloads.psl.noaa.gov/Datasets/cpc_global_precip/)), and PERCCDR can be freely accessed  
484 through the Center for Hydrometeorology and Remote Sensing (CHRS; <https://chrsdata.eng.uci.edu/>).

#### 486 **Author contribution**

487 SG, JL, and SJD conceived the study, incorporating input from all co-authors. SG led the global hydrological  
488 modelling, while JL, SJD, and LS assisted with data management and computational resources. SG was  
489 responsible for evaluating various precipitation datasets for hydrological modelling and drafted the initial  
490 manuscript. SC provided the hydrological model and input parameters. MW, GB, RB, PD, HG, EV, YL, RH, LH,  
491 SM, and JN executed extensive data quality control and identified stations for evaluation. PA, HC, AN, AT, and  
492 JS provided code, methods, and guidance. DP, SJD, and SED supervised the research and secured funding. All  
493 authors contributed to investigating research findings and played integral roles in manuscript writing and editing.

#### 494 **Competing interests**

495 We declare that Louise Slater is a topical editor of Hydrology and Earth System Sciences (HESS).

#### 496 **Acknowledgements**

497 This work is part of the Evolution of Global Flood Hazard and Risk (EVOFLOOD) project [NE/S015817/1]  
498 supported by the Natural Environment Research Council (NERC), the UK Foreign, Commonwealth and  
499 Development Office (FCDO) for the benefit of developing countries (Programme Code 201880) and the UK's  
500 Natural Environment Research Council (NERC; NE/S017380/1).

501

502

503

504

505

506

507

508

509

510

511

512

513 Reference

- 514 Abatzoglou, J. T., Dobrowski, S. Z., Parks, S. A., and Hegewisch, K. C.: TerraClimate, a high-resolution global  
515 dataset of monthly climate and climatic water balance from 1958–2015, *Sci Data*, 5, 170191,  
516 <https://doi.org/10.1038/sdata.2017.191>, 2018.
- 517 Acharya, S. C., Nathan, R., Wang, Q. J., Su, C.-H., and Eizenberg, N.: An evaluation of daily precipitation from  
518 a regional atmospheric reanalysis over Australia, *Hydrology and Earth System Sciences*, 23, 3387–3403,  
519 <https://doi.org/10.5194/hess-23-3387-2019>, 2019.
- 520 Ahmed, K., Shahid, S., Wang, X., Nawaz, N., and Khan, N.: Evaluation of Gridded Precipitation Datasets over  
521 Arid Regions of Pakistan, *Water*, 11, 210, <https://doi.org/10.3390/w11020210>, 2019.
- 522 Alazzy, A. A., Lü, H., Chen, R., Ali, A. B., Zhu, Y., and Su, J.: Evaluation of Satellite Precipitation Products  
523 and Their Potential Influence on Hydrological Modeling over the Ganzi River Basin of the Tibetan Plateau,  
524 *Advances in Meteorology*, 2017, e3695285, <https://doi.org/10.1155/2017/3695285>, 2017.
- 525 AL-Falahi, A. H., Saddique, N., Spank, U., Gebrechorkos, S. H., and Bernhofer, C.: Evaluation the Performance  
526 of Several Gridded Precipitation Products over the Highland Region of Yemen for Water Resources  
527 Management, *Remote Sensing*, 12, 2984, <https://doi.org/10.3390/rs12182984>, 2020.
- 528 Araujo Palharini, R. S., Vila, D. A., Rodrigues, D. T., Palharini, R. C., Mattos, E. V., and Pedra, G. U.:  
529 Assessment of extreme rainfall estimates from satellite-based: Regional analysis, *Remote Sensing Applications:  
530 Society and Environment*, 23, 100603, <https://doi.org/10.1016/j.rsase.2021.100603>, 2021.
- 531 Bárdossy, A., Kilsby, C., Birkinshaw, S., Wang, N., and Anwar, F.: Is Precipitation Responsible for the Most  
532 Hydrological Model Uncertainty?, *Frontiers in Water*, 4, 2022.
- 533 Bechtold, P., R Forbes, I Sandu, S Lang, and M Ahlgrimm: A major moist physics upgrade for the IFS, , 24–32,  
534 2020.
- 535 Beck, H. E., Vergopolan, N., Pan, M., Levizzani, V., Dijk, A. I. J. M. van, Weedon, G. P., Brocca, L.,  
536 Pappenberger, F., Huffman, G. J., and Wood, E. F.: Global-scale evaluation of 22 precipitation datasets using  
537 gauge observations and hydrological modeling, *Hydrology and Earth System Sciences*, 21, 6201–6217,  
538 <https://doi.org/10.5194/hess-21-6201-2017>, 2017a.
- 539 Beck, H. E., van Dijk, A. I. J. M., Levizzani, V., Schellekens, J., Miralles, D. G., Martens, B., and de Roo, A.:  
540 MSWEP: 3-hourly 0.25° global gridded precipitation (1979–2015) by merging gauge, satellite, and reanalysis  
541 data, *Hydrology and Earth System Sciences*, 21, 589–615, <https://doi.org/10.5194/hess-21-589-2017>, 2017b.
- 542 Beck, H. E., Pan, M., Roy, T., Weedon, G. P., Pappenberger, F., van Dijk, A. I. J. M., Huffman, G. J., Adler, R.  
543 F., and Wood, E. F.: Daily evaluation of 26 precipitation datasets using Stage-IV gauge-radar data for the  
544 CONUS, *Hydrology and Earth System Sciences*, 23, 207–224, <https://doi.org/10.5194/hess-23-207-2019>,  
545 2019a.
- 546 Beck, H. E., Wood, E. F., Pan, M., Fisher, C. K., Miralles, D. G., Dijk, A. I. J. M. van, McVicar, T. R., and  
547 Adler, R. F.: MSWEP V2 Global 3-Hourly 0.1° Precipitation: Methodology and Quantitative Assessment,  
548 *Bulletin of the American Meteorological Society*, 100, 473–500, <https://doi.org/10.1175/BAMS-D-17-0138.1>,  
549 2019b.
- 550 Brunner, M. I., Slater, L., Tallaksen, L. M., and Clark, M.: Challenges in modeling and predicting floods and  
551 droughts: A review, *WIREs Water*, 8, e1520, <https://doi.org/10.1002/wat2.1520>, 2021.
- 552 Chen, M., Shi, W., Xie, P., Silva, V. B. S., Kousky, V. E., Wayne Higgins, R., and Janowiak, J. E.: Assessing  
553 objective techniques for gauge-based analyses of global daily precipitation, *Journal of Geophysical Research:  
554 Atmospheres*, 113, <https://doi.org/10.1029/2007JD009132>, 2008.

- 555 Chen, Y., Hu, D., Duan, X., Zhang, Y., Liu, M., and Shasha, W.: Rainfall-runoff simulation and flood dynamic  
556 monitoring based on CHIRPS and MODIS-ET, *International Journal of Remote Sensing*, 41, 4206–4225,  
557 <https://doi.org/10.1080/01431161.2020.1714779>, 2020.
- 558 Cohen, S., Kettner, A. J., Syvitski, J. P. M., and Fekete, B. M.: WBMsed, a distributed global-scale riverine  
559 sediment flux model: Model description and validation, *Computers & Geosciences*, 53, 80–93,  
560 <https://doi.org/10.1016/j.cageo.2011.08.011>, 2013.
- 561 Cohen, S., Kettner, A. J., and Syvitski, J. P. M.: Global suspended sediment and water discharge dynamics  
562 between 1960 and 2010: Continental trends and intra-basin sensitivity, *Global and Planetary Change*, 115, 44–  
563 58, <https://doi.org/10.1016/j.gloplacha.2014.01.011>, 2014.
- 564 Cohen, S., Syvitski, J., Ashley, T., Lammers, R., Fekete, B., and Li, H.-Y.: Spatial Trends and Drivers of  
565 Bedload and Suspended Sediment Fluxes in Global Rivers, *Water Resources Research*, 58, e2021WR031583,  
566 <https://doi.org/10.1029/2021WR031583>, 2022.
- 567 Day, C. A. and Howarth, D. A.: Modeling Climate Change Impacts on the Water Balance of a Medium-Scale  
568 Mixed-Forest Watershed, SE USA, *Southeastern Geographer*, 59, 110–129, 2019.
- 569 Dembélé, M., Schaeffli, B., van de Giesen, N., and Mariéthoz, G.: Suitability of 17 gridded rainfall and  
570 temperature datasets for large-scale hydrological modelling in West Africa, *Hydrology and Earth System  
571 Sciences*, 24, 5379–5406, <https://doi.org/10.5194/hess-24-5379-2020>, 2020.
- 572 Dunn, F. E., Darby, S. E., Nicholls, R. J., Cohen, S., Zarfl, C., and Fekete, B. M.: Projections of declining  
573 fluvial sediment delivery to major deltas worldwide in response to climate change and anthropogenic stress,  
574 *Environ. Res. Lett.*, 14, 084034, <https://doi.org/10.1088/1748-9326/ab304e>, 2019.
- 575 Eini, M. R., Rahmati, A., and Piniewski, M.: Hydrological application and accuracy evaluation of PERSIANN  
576 satellite-based precipitation estimates over a humid continental climate catchment, *Journal of Hydrology:  
577 Regional Studies*, 41, 101109, <https://doi.org/10.1016/j.ejrh.2022.101109>, 2022.
- 578 El Kenawy, A. M., Lopez-Moreno, J. I., McCabe, M. F., and Vicente-Serrano, S. M.: Evaluation of the TMPA-  
579 3B42 precipitation product using a high-density rain gauge network over complex terrain in northeastern Iberia,  
580 *Global and Planetary Change*, 133, 188–200, <https://doi.org/10.1016/j.gloplacha.2015.08.013>, 2015.
- 581 Fallah, A., Rakhshandehroo, G. R., Berg, P., O, S., and Orth, R.: Evaluation of precipitation datasets against  
582 local observations in southwestern Iran, *International Journal of Climatology*, 40, 4102–4116,  
583 <https://doi.org/10.1002/joc.6445>, 2020.
- 584 Funk, C., Peterson, P., Landsfeld, M., Pedreros, D., Verdin, J., Shukla, S., Husak, G., Rowland, J., Harrison, L.,  
585 Hoell, A., and Michaelsen, J.: The climate hazards infrared precipitation with stations—a new environmental  
586 record for monitoring extremes, *Scientific Data*, 2, 150066, <https://doi.org/10.1038/sdata.2015.66>, 2015.
- 587 Gebrechorkos, S. H., Hülsmann, S., and Bernhofer, C.: Evaluation of multiple climate data sources for  
588 managing environmental resources in East Africa, *Hydrology and Earth System Sciences*, 22, 4547–4564,  
589 <https://doi.org/10.5194/hess-22-4547-2018>, 2018.
- 590 Gebrechorkos, S. H., Bernhofer, C., and Hülsmann, S.: Impacts of projected change in climate on water balance  
591 in basins of East Africa, *Science of The Total Environment*, <https://doi.org/10.1016/j.scitotenv.2019.05.053>,  
592 2019.
- 593 Gebrechorkos, S. H., Bernhofer, C., and Hülsmann, S.: Climate change impact assessment on the hydrology of a  
594 large river basin in Ethiopia using a local-scale climate modelling approach, *Science of The Total Environment*,  
595 742, 140504, <https://doi.org/10.1016/j.scitotenv.2020.140504>, 2020.
- 596 Gebrechorkos, S. H., Leyland, J., Darby, S., and Parsons, D.: High-resolution daily global climate dataset of  
597 BCCAQ statistically downscaled CMIP6 models for the EVOFLOOD project. NERC EDS Centre for  
598 Environmental Data Analysis, <https://doi.org/10.5285/C107618F1DB34801BB88A1E927B82317>, 2022a.

- 599 Gebrechorkos, S. H., Pan, M., Beck, H. E., and Sheffield, J.: Performance of State-of-the-Art C3S European  
600 Seasonal Climate Forecast Models for Mean and Extreme Precipitation Over Africa, *Water Resources Research*,  
601 58, e2021WR031480, <https://doi.org/10.1029/2021WR031480>, 2022b.
- 602 Gebrechorkos, S. H., Pan, M., Lin, P., Anghileri, D., Forsythe, N., Pritchard, D. M. W., Fowler, H. J., Obuobie,  
603 E., Darko, D., and Sheffield, J.: Variability and changes in hydrological drought in the Volta Basin, West  
604 Africa, *Journal of Hydrology: Regional Studies*, 42, 101143, <https://doi.org/10.1016/j.ejrh.2022.101143>, 2022c.
- 605 Gebrechorkos, S. H., Peng, J., Dyer, E., Miralles, D. G., Vicente-Serrano, S. M., Funk, C., Beck, H. E., Asfaw,  
606 D. T., Singer, M. B., and Dadson, S. J.: Global High-Resolution Drought Indices for 1981–2022, *Earth  
607 System Science Data Discussions*, 1–28, <https://doi.org/10.5194/essd-2023-276>, 2023.
- 608 Geleta, C. D. and Deressa, T. A.: Evaluation of Climate Hazards Group InfraRed Precipitation Station  
609 (CHIRPS) satellite-based rainfall estimates over Finchaa and Neshe Watersheds, Ethiopia, *Engineering Reports*,  
610 3, e12338, <https://doi.org/10.1002/eng2.12338>, 2021.
- 611 GRDC: The Global Runoff Data Centre, 56068 Koblenz, Germany, 2023.
- 612 Grogan, D. S., Zuidema, S., Prusevich, A., Wollheim, W. M., Glidden, S., and Lammers, R. B.: Water balance  
613 model (WBM) v.1.0.0: a scalable gridded global hydrologic model with water-tracking functionality,  
614 *Geoscientific Model Development*, 15, 7287–7323, <https://doi.org/10.5194/gmd-15-7287-2022>, 2022.
- 615 Gu, L., Yin, J., Wang, S., Chen, J., Qin, H., Yan, X., He, S., and Zhao, T.: How well do the multi-satellite and  
616 atmospheric reanalysis products perform in hydrological modelling, *Journal of Hydrology*, 617, 128920,  
617 <https://doi.org/10.1016/j.jhydrol.2022.128920>, 2023.
- 618 Guo, B., Zhang, J., Xu, T., Croke, B., Jakeman, A., Song, Y., Yang, Q., Lei, X., and Liao, W.: Applicability  
619 Assessment and Uncertainty Analysis of Multi-Precipitation Datasets for the Simulation of Hydrologic Models,  
620 *Water*, 10, 1611, <https://doi.org/10.3390/w10111611>, 2018.
- 621 Gupta, H. V., Kling, H., Yilmaz, K. K., and Martinez, G. F.: Decomposition of the mean squared error and NSE  
622 performance criteria: Implications for improving hydrological modelling, *Journal of Hydrology*, 377, 80–91,  
623 <https://doi.org/10.1016/j.jhydrol.2009.08.003>, 2009.
- 624 Hafizi, H. and Sorman, A. A.: Assessment of 13 Gridded Precipitation Datasets for Hydrological Modeling in a  
625 Mountainous Basin, *Atmosphere*, 13, 143, <https://doi.org/10.3390/atmos13010143>, 2022.
- 626 Harrigan, S., Zsoter, E., Alfieri, L., Prudhomme, C., Salamon, P., Wetterhall, F., Barnard, C., Cloke, H., and  
627 Pappenberger, F.: GloFAS-ERA5 operational global river discharge reanalysis 1979–present, *Earth System  
628 Science Data*, 12, 2043–2060, <https://doi.org/10.5194/essd-12-2043-2020>, 2020.
- 629 He, Q., Shen, Z., Wan, M., and Li, L.: Precipitable Water Vapor Converted from GNSS-ZTD and ERA5  
630 Datasets for the Monitoring of Tropical Cyclones, *IEEE Access*, 8, 87275–87290,  
631 <https://doi.org/10.1109/ACCESS.2020.2991094>, 2020.
- 632 Her, Y., Yoo, S.-H., Cho, J., Hwang, S., Jeong, J., and Seong, C.: Uncertainty in hydrological analysis of  
633 climate change: multi-parameter vs. multi-GCM ensemble predictions, *Sci Rep*, 9, 4974,  
634 <https://doi.org/10.1038/s41598-019-41334-7>, 2019.
- 635 Hersbach, H., Bell, B., Berrisford, P., Hirahara, S., Horányi, A., Muñoz-Sabater, J., Nicolas, J., Peubey, C.,  
636 Radu, R., Schepers, D., Simmons, A., Soci, C., Abdalla, S., Abellan, X., Balsamo, G., Bechtold, P., Biavati, G.,  
637 Bidlot, J., Bonavita, M., De Chiara, G., Dahlgren, P., Dee, D., Diamantakis, M., Dragani, R., Flemming, J.,  
638 Forbes, R., Fuentes, M., Geer, A., Haimberger, L., Healy, S., Hogan, R. J., Hólm, E., Janisková, M., Keeley, S.,  
639 Laloyaux, P., Lopez, P., Lupu, C., Radnoti, G., de Rosnay, P., Rozum, I., Vamborg, F., Villaume, S., and  
640 Thépaut, J.-N.: The ERA5 global reanalysis, *Quarterly Journal of the Royal Meteorological Society*, 146, 1999–  
641 2049, <https://doi.org/10.1002/qj.3803>, 2020.
- 642 Hong, Y., Xuan Do, H., Kessler, J., Fry, L., Read, L., Rafieei Nasab, A., Gronewold, A. D., Mason, L., and  
643 Anderson, E. J.: Evaluation of gridded precipitation datasets over international basins and large lakes, *Journal of  
644 Hydrology*, 607, 127507, <https://doi.org/10.1016/j.jhydrol.2022.127507>, 2022.

- 645 Hou, D., Charles, M., Luo, Y., Toth, Z., Zhu, Y., Krzysztofowicz, R., Lin, Y., Xie, P., Seo, D.-J., Pena, M., and  
646 Cui, B.: Climatology-Calibrated Precipitation Analysis at Fine Scales: Statistical Adjustment of Stage IV toward  
647 CPC Gauge-Based Analysis, *Journal of Hydrometeorology*, 15, 2542–2557, <https://doi.org/10.1175/JHM-D-11-0140.1>, 2014.
- 649 Huang, Z., Zhang, Y., Xu, J., Fang, X., and Ma, Z.: Can satellite precipitation estimates capture the magnitude  
650 of extreme rainfall Events?, *Remote Sensing Letters*, 13, 1048–1057,  
651 <https://doi.org/10.1080/2150704X.2022.2123258>, 2022.
- 652 van Huijgevoort, M. H. J., Hazenberg, P., van Lanen, H. a. J., Teuling, A. J., Clark, D. B., Folwell, S., Gosling,  
653 S. N., Hanasaki, N., Heinke, J., Koirala, S., Stacke, T., Voss, F., Sheffield, J., and Uijlenhoet, R.: Global  
654 Multimodel Analysis of Drought in Runoff for the Second Half of the Twentieth Century, *J. Hydrometeor.*, 14,  
655 1535–1552, <https://doi.org/10.1175/JHM-D-12-0186.1>, 2013.
- 656 Ibrahim, A. H., Molla, D. D., and Lohani, T. K.: Performance evaluation of satellite-based rainfall estimates for  
657 hydrological modeling over Bilate river basin, Ethiopia, *World Journal of Engineering*, ahead-of-print,  
658 <https://doi.org/10.1108/WJE-03-2022-0106>, 2022.
- 659 Jiang, Q., Li, W., Wen, J., Fan, Z., Chen, Y., Scaioni, M., and Wang, J.: Evaluation of satellite-based products  
660 for extreme rainfall estimations in the eastern coastal areas of China, *Journal of Integrative Environmental  
661 Sciences*, 16, 191–207, <https://doi.org/10.1080/1943815X.2019.1707233>, 2019.
- 662 Jiang, S., Wei, L., Ren, L., Zhang, L., Wang, M., and Cui, H.: Evaluation of IMERG, TMPA, ERA5, and CPC  
663 precipitation products over mainland China: Spatiotemporal patterns and extremes, *Water Science and  
664 Engineering*, 16, 45–56, <https://doi.org/10.1016/j.wse.2022.05.001>, 2023.
- 665 Jiao, D., Xu, N., Yang, F., and Xu, K.: Evaluation of spatial-temporal variation performance of ERA5  
666 precipitation data in China, *Sci Rep*, 11, 17956, <https://doi.org/10.1038/s41598-021-97432-y>, 2021.
- 667 Kidd, C. and Levizzani, V.: Status of satellite precipitation retrievals, *Hydrology and Earth System Sciences*, 15,  
668 1109–1116, <https://doi.org/10.5194/hess-15-1109-2011>, 2011.
- 669 Kidd, C., Becker, A., Huffman, G. J., Muller, C. L., Joe, P., Skofronick-Jackson, G., and Kirschbaum, D. B.: So,  
670 How Much of the Earth’s Surface Is Covered by Rain Gauges?, *Bulletin of the American Meteorological  
671 Society*, 98, 69–78, <https://doi.org/10.1175/BAMS-D-14-00283.1>, 2017.
- 672 Knoben, W. J. M., Freer, J. E., and Woods, R. A.: Technical note: Inherent benchmark or not? Comparing  
673 Nash–Sutcliffe and Kling–Gupta efficiency scores, *Hydrology and Earth System Sciences*, 23, 4323–4331,  
674 <https://doi.org/10.5194/hess-23-4323-2019>, 2019.
- 675 Laiti, L., Mallucci, S., Piccolroaz, S., Bellin, A., Zardi, D., Fiori, A., Nikulin, G., and Majone, B.: Testing the  
676 Hydrological Coherence of High-Resolution Gridded Precipitation and Temperature Data Sets, *Water Resources  
677 Research*, 54, 1999–2016, <https://doi.org/10.1002/2017WR021633>, 2018.
- 678 Lakew, H. B.: Investigating the effectiveness of bias correction and merging MSWEP with gauged rainfall for  
679 the hydrological simulation of the upper Blue Nile basin, *Journal of Hydrology: Regional Studies*, 32, 100741,  
680 <https://doi.org/10.1016/j.ejrh.2020.100741>, 2020.
- 681 Lavers, D. A., Harrigan, S., and Prudhomme, C.: Precipitation Biases in the ECMWF Integrated Forecasting  
682 System, *Journal of Hydrometeorology*, 22, 1187–1198, <https://doi.org/10.1175/JHM-D-20-0308.1>, 2021.
- 683 Lavers, D. A., Simmons, A., Vamborg, F., and Rodwell, M. J.: An evaluation of ERA5 precipitation for climate  
684 monitoring, *Quarterly Journal of the Royal Meteorological Society*, 148, 3152–3165,  
685 <https://doi.org/10.1002/qj.4351>, 2022.
- 686 Lehner, B., Verdin, K. L., and Jarvis, A.: New global hydrography derived from spaceborne elevation data, *Eos,  
687 Transactions, American Geophysical Union*, 89, 2, <https://doi.org/10.1029/2008EO100001>, 2008.
- 688 Lehner, B., Liermann, C. R., Revenga, C., Vörösmarty, C., Fekete, B., Crouzet, P., Döll, P., Endejan, M.,  
689 Frenken, K., Magome, J., Nilsson, C., Robertson, J. C., Rödel, R., Sindorf, N., and Wisser, D.: High-resolution

690 mapping of the world's reservoirs and dams for sustainable river-flow management, *Frontiers in Ecology and*  
691 *the Environment*, 9, 494–502, <https://doi.org/10.1890/100125>, 2011.

692 Li, L., Wang, Y., Wang, L., Hu, Q., Zhu, Z., Li, L., and Li, C.: Spatio-temporal accuracy evaluation of MSWEP  
693 daily precipitation over the Huaihe River Basin, China: A comparison study with representative satellite- and  
694 reanalysis-based products, *J. Geogr. Sci.*, 32, 2271–2290, <https://doi.org/10.1007/s11442-022-2047-9>, 2022a.

695 Li, M., Lv, X., Zhu, L., Uchenna Ochege, F., and Guo, H.: Evaluation and Application of MSWEP in Drought  
696 Monitoring in Central Asia, *Atmosphere*, 13, 1053, <https://doi.org/10.3390/atmos13071053>, 2022b.

697 Lin, P., Pan, M., Beck, H. E., Yang, Y., Yamazaki, D., Frasson, R., David, C. H., Durand, M., Pavelsky, T. M.,  
698 Allen, G. H., Gleason, C. J., and Wood, E. F.: Global Reconstruction of Naturalized River Flows at 2.94 Million  
699 Reaches, *Water Resources Research*, 55, 6499–6516, <https://doi.org/10.1029/2019WR025287>, 2019.

700 López López, P., Sutanudjaja, E. H., Schellekens, J., Sterk, G., and Bierkens, M. F. P.: Calibration of a large-  
701 scale hydrological model using satellite-based soil moisture and evapotranspiration products, *Hydrology and*  
702 *Earth System Sciences*, 21, 3125–3144, <https://doi.org/10.5194/hess-21-3125-2017>, 2017.

703 Luo, X., Wu, W., He, D., Li, Y., and Ji, X.: Hydrological Simulation Using TRMM and CHIRPS Precipitation  
704 Estimates in the Lower Lancang-Mekong River Basin, *Chin. Geogr. Sci.*, 29, 13–25,  
705 <https://doi.org/10.1007/s11769-019-1014-6>, 2019.

706 Maggioni, V. and Massari, C.: On the performance of satellite precipitation products in riverine flood modeling:  
707 A review, *Journal of Hydrology*, 558, 214–224, <https://doi.org/10.1016/j.jhydrol.2018.01.039>, 2018.

708 Mazzoleni, M., Brandimarte, L., and Amaranto, A.: Evaluating precipitation datasets for large-scale distributed  
709 hydrological modelling, *Journal of Hydrology*, 578, 124076, <https://doi.org/10.1016/j.jhydrol.2019.124076>,  
710 2019.

711 Mehran, A. and AghaKouchak, A.: Capabilities of satellite precipitation datasets to estimate heavy precipitation  
712 rates at different temporal accumulations, *Hydrological Processes*, 28, 2262–2270,  
713 <https://doi.org/10.1002/hyp.9779>, 2014.

714 Menne, M. J., Durre, I., Vose, R. S., Gleason, B. E., and Houston, T. G.: An Overview of the Global Historical  
715 Climatology Network-Daily Database, *Journal of Atmospheric and Oceanic Technology*, 29, 897–910,  
716 <https://doi.org/10.1175/JTECH-D-11-00103.1>, 2012.

717 Mianabadi, A., Salari, K., and Pourmohamad, Y.: Drought monitoring using the long-term CHIRPS  
718 precipitation over Southeastern Iran, *Appl Water Sci*, 12, 183, <https://doi.org/10.1007/s13201-022-01705-4>,  
719 2022.

720 Miao, C., Ashouri, H., Hsu, K.-L., Sorooshian, S., and Duan, Q.: Evaluation of the PERSIANN-CDR Daily  
721 Rainfall Estimates in Capturing the Behavior of Extreme Precipitation Events over China, *Journal of*  
722 *Hydrometeorology*, 16, 1387–1396, <https://doi.org/10.1175/JHM-D-14-0174.1>, 2015.

723 Miao, Q., Pan, B., Wang, H., Hsu, K., and Sorooshian, S.: Improving Monsoon Precipitation Prediction Using  
724 Combined Convolutional and Long Short Term Memory Neural Network, *Water*, 11, 977,  
725 <https://doi.org/10.3390/w11050977>, 2019.

726 Michaelides, S., Levizzani, V., Anagnostou, E., Bauer, P., Kasparis, T., and Lane, J. E.: Precipitation:  
727 Measurement, remote sensing, climatology and modeling, *Atmospheric Research*, 94, 512–533,  
728 <https://doi.org/10.1016/j.atmosres.2009.08.017>, 2009.

729 Moazami, S., Golian, S., Kavianpour, M. R., and Hong, Y.: Comparison of PERSIANN and V7 TRMM Multi-  
730 satellite Precipitation Analysis (TMPA) products with rain gauge data over Iran, *International Journal of Remote*  
731 *Sensing*, 34, 8156–8171, <https://doi.org/10.1080/01431161.2013.833360>, 2013.

732 Moragoda, N. and Cohen, S.: Climate-induced trends in global riverine water discharge and suspended sediment  
733 dynamics in the 21st century, *Global and Planetary Change*, 191, 103199,  
734 <https://doi.org/10.1016/j.gloplacha.2020.103199>, 2020.

- 735 Nguyen, P., Thorstensen, A., Sorooshian, S., Hsu, K., Aghakouchak, A., Ashouri, H., Tran, H., and Braithwaite,  
736 D.: Global Precipitation Trends across Spatial Scales Using Satellite Observations, *Bulletin of the American  
737 Meteorological Society*, 99, 689–697, <https://doi.org/10.1175/BAMS-D-17-0065.1>, 2018.
- 738 Opere, A. O., Waswa, R., and Mutua, F. M.: Assessing the Impacts of Climate Change on Surface Water  
739 Resources Using WEAP Model in Narok County, Kenya, *Frontiers in Water*, 3, 2022.
- 740 Palharini, R. S. A., Vila, D. A., Rodrigues, D. T., Quispe, D. P., Palharini, R. C., de Siqueira, R. A., and de  
741 Sousa Afonso, J. M.: Assessment of the Extreme Precipitation by Satellite Estimates over South America,  
742 *Remote Sensing*, 12, 2085, <https://doi.org/10.3390/rs12132085>, 2020.
- 743 Parker, W. S.: Reanalyses and Observations: What’s the Difference?, *Bulletin of the American Meteorological  
744 Society*, 97, 1565–1572, <https://doi.org/10.1175/BAMS-D-14-00226.1>, 2016.
- 745 Peng, J., Dadson, S., Hirpa, F., Dyer, E., Lees, T., Miralles, D. G., Vicente-Serrano, S. M., and Funk, C.: A pan-  
746 African high-resolution drought index dataset, *Earth System Science Data*, 12, 753–769,  
747 <https://doi.org/10.5194/essd-12-753-2020>, 2020.
- 748 Raimonet, M., Oudin, L., Thieu, V., Silvestre, M., Vautard, R., Rabouille, C., and Moigne, P. L.: Evaluation of  
749 Gridded Meteorological Datasets for Hydrological Modeling, *Journal of Hydrometeorology*, 18, 3027–3041,  
750 <https://doi.org/10.1175/JHM-D-17-0018.1>, 2017.
- 751 Reichle, R. H., Koster, R. D., Lannoy, G. J. M. D., Forman, B. A., Liu, Q., Mahanama, S. P. P., and Touré, A.:  
752 Assessment and Enhancement of MERRA Land Surface Hydrology Estimates, *Journal of Climate*, 24, 6322–  
753 6338, <https://doi.org/10.1175/JCLI-D-10-05033.1>, 2011.
- 754 Reis, A. A. dos, Weerts, A., Ramos, M.-H., Wetterhall, F., and Fernandes, W. dos S.: Hydrological data and  
755 modeling to combine and validate precipitation datasets relevant to hydrological applications, *Journal of  
756 Hydrology: Regional Studies*, 44, 101200, <https://doi.org/10.1016/j.ejrh.2022.101200>, 2022.
- 757 Sadeghi, M., Nguyen, P., Naeini, M. R., Hsu, K., Braithwaite, D., and Sorooshian, S.: PERSIANN-CCS-CDR, a  
758 3-hourly 0.04° global precipitation climate data record for heavy precipitation studies, *Sci Data*, 8, 157,  
759 <https://doi.org/10.1038/s41597-021-00940-9>, 2021.
- 760 Salehi, H., Sadeghi, M., Golian, S., Nguyen, P., Murphy, C., and Sorooshian, S.: The Application of  
761 PERSIANN Family Datasets for Hydrological Modeling, *Remote Sensing*, 14, 3675,  
762 <https://doi.org/10.3390/rs14153675>, 2022.
- 763 Satgé, F., Ruelland, D., Bonnet, M.-P., Molina, J., and Pillco, R.: Consistency of satellite-based precipitation  
764 products in space and over time compared with gauge observations and snow- hydrological modelling in the  
765 Lake Titicaca region, *Hydrology and Earth System Sciences*, 23, 595–619, [https://doi.org/10.5194/hess-23-595-  
766 2019](https://doi.org/10.5194/hess-23-595-2019), 2019.
- 767 Seyyedi, H., Anagnostou, E. N., Beighley, E., and McCollum, J.: Hydrologic evaluation of satellite and  
768 reanalysis precipitation datasets over a mid-latitude basin, *Atmospheric Research*, 164–165, 37–48,  
769 <https://doi.org/10.1016/j.atmosres.2015.03.019>, 2015.
- 770 Shaowei, N., Jie, W., Juliang, J., Xiaoyan, X., Yuliang, Z., Fan, S., and Linlin, Z.: Comprehensive evaluation of  
771 satellite-derived precipitation products considering spatial distribution difference of daily precipitation over  
772 eastern China, *Journal of Hydrology: Regional Studies*, 44, 101242, <https://doi.org/10.1016/j.ejrh.2022.101242>,  
773 2022.
- 774 Sheffield, J., Goteti, G., and Wood, E. F.: Development of a 50-Year High-Resolution Global Dataset of  
775 Meteorological Forcings for Land Surface Modeling, *J. Climate*, 19, 3088–3111,  
776 <https://doi.org/10.1175/JCLI3790.1>, 2006.
- 777 Sheffield, J., Wood, E. F., Pan, M., Beck, H., Coccia, G., Serrat-Capdevila, A., and Verbist, K.: Satellite Remote  
778 Sensing for Water Resources Management: Potential for Supporting Sustainable Development in Data-Poor  
779 Regions, *Water Resources Research*, 54, 9724–9758, <https://doi.org/10.1029/2017WR022437>, 2018.

- 780 Shen, Y., Xiong, A., Wang, Y., and Xie, P.: Performance of high-resolution satellite precipitation products over  
781 China, *Journal of Geophysical Research: Atmospheres*, 115, <https://doi.org/10.1029/2009JD012097>, 2010.
- 782 Solakian, J., Maggioni, V., and Godrej, A. N.: On the Performance of Satellite-Based Precipitation Products in  
783 Simulating Streamflow and Water Quality During Hydrometeorological Extremes, *Frontiers in Environmental*  
784 *Science*, 8, 2020.
- 785 Sun, G., Wei, Y., Wang, G., Shi, R., Chen, H., and Mo, C.: Downscaling Correction and Hydrological  
786 Applicability of the Three Latest High-Resolution Satellite Precipitation Products (GPM, GSMAP, and  
787 MSWEP) in the Pingtang Catchment, China, *Advances in Meteorology*, 2022, e6507109,  
788 <https://doi.org/10.1155/2022/6507109>, 2022.
- 789 Sun, Q., Miao, C., Duan, Q., Ashouri, H., Sorooshian, S., and Hsu, K.-L.: A Review of Global Precipitation  
790 Data Sets: Data Sources, Estimation, and Intercomparisons, *Reviews of Geophysics*, 56, 79–107,  
791 <https://doi.org/10.1002/2017RG000574>, 2018.
- 792 Tang, X., Zhang, J., Gao, C., Ruben, G. B., and Wang, G.: Assessing the Uncertainties of Four Precipitation  
793 Products for Swat Modeling in Mekong River Basin, *Remote Sensing*, 11, 304,  
794 <https://doi.org/10.3390/rs11030304>, 2019.
- 795 Ursulak, J. and Coulibaly, P.: Integration of hydrological models with entropy and multi-objective optimization  
796 based methods for designing specific needs streamflow monitoring networks, *Journal of Hydrology*, 593,  
797 125876, <https://doi.org/10.1016/j.jhydrol.2020.125876>, 2021.
- 798 Voisin, N., Wood, A. W., and Lettenmaier, D. P.: Evaluation of Precipitation Products for Global Hydrological  
799 Prediction, *Journal of Hydrometeorology*, 9, 388–407, <https://doi.org/10.1175/2007JHM938.1>, 2008.
- 800 Wang, M., Rezaie-Balf, M., Naganna, S. R., and Yaseen, Z. M.: Sourcing CHIRPS precipitation data for  
801 streamflow forecasting using intrinsic time-scale decomposition based machine learning models, *Hydrological*  
802 *Sciences Journal*, 66, 1437–1456, <https://doi.org/10.1080/02626667.2021.1928138>, 2021.
- 803 Wang, N., Liu, W., Sun, F., Yao, Z., Wang, H., and Liu, W.: Evaluating satellite-based and reanalysis  
804 precipitation datasets with gauge-observed data and hydrological modeling in the Xihe River Basin, China,  
805 *Atmospheric Research*, 234, 104746, <https://doi.org/10.1016/j.atmosres.2019.104746>, 2020.
- 806 Wati, T., Hadi, T. W., Sopaheluwakan, A., and Hutasoit, L. M.: Statistics of the Performance of Gridded  
807 Precipitation Datasets in Indonesia, *Advances in Meteorology*, 2022, e7995761,  
808 <https://doi.org/10.1155/2022/7995761>, 2022.
- 809 Wisser, D., Fekete, B. M., Vörösmarty, C. J., and Schumann, A. H.: Reconstructing 20th century global  
810 hydrography: a contribution to the Global Terrestrial Network- Hydrology (GTN-H), *Hydrology and Earth*  
811 *System Sciences*, 14, 1–24, <https://doi.org/10.5194/hess-14-1-2010>, 2010.
- 812 Wollheim, W. M., Vörösmarty, C. J., Bouwman, A. F., Green, P., Harrison, J., Linder, E., Peterson, B. J.,  
813 Seitzinger, S. P., and Syvitski, J. P. M.: Global N removal by freshwater aquatic systems using a spatially  
814 distributed, within-basin approach, *Global Biogeochemical Cycles*, 22, <https://doi.org/10.1029/2007GB002963>,  
815 2008.
- 816 Wu, Z., Xu, Z., Wang, F., He, H., Zhou, J., Wu, X., and Liu, Z.: Hydrologic Evaluation of Multi-Source  
817 Satellite Precipitation Products for the Upper Huaihe River Basin, China, *Remote Sensing*, 10, 840,  
818 <https://doi.org/10.3390/rs10060840>, 2018.
- 819 Xiang, Y., Chen, J., Li, L., Peng, T., and Yin, Z.: Evaluation of Eight Global Precipitation Datasets in  
820 Hydrological Modeling, *Remote Sensing*, 13, 2831, <https://doi.org/10.3390/rs13142831>, 2021.
- 821 Zambrano-Bigiarini, M., Nauditt, A., Birkel, C., Verbist, K., and Ribbe, L.: Temporal and spatial evaluation of  
822 satellite-based rainfall estimates across the complex topographical and climatic gradients of Chile, *Hydrology*  
823 *and Earth System Sciences Discussions*, 1–43, <https://doi.org/10.5194/hess-2016-453>, 2016.

824 Zhu, D., Ilyas, A. M., Wang, G., and Zeng, B.: Long-term hydrological assessment of remote sensing  
825 precipitation from multiple sources over the lower Yangtze River basin, China, *Meteorological Applications*, 28,  
826 e1991, <https://doi.org/10.1002/met.1991>, 2021.

827 Zhu, H., Li, Y., Huang, Y., Li, Y., Hou, C., and Shi, X.: Evaluation and hydrological application of satellite-  
828 based precipitation datasets in driving hydrological models over the Huifa river basin in Northeast China,  
829 *Atmospheric Research*, 207, 28–41, <https://doi.org/10.1016/j.atmosres.2018.02.022>, 2018.

830